BNL-68037

AIRBORNE CH_2O MEASUREMENTS OVER THE NORTH ATLANTIC DURING THE 1997 NARE CAMPAIGN: INSTRUMENT COMPARISONS AND DISTRIBUTIONS

Alan Fried[1], Yin-Nan Lee[2], Greg Frost[3,4], Bryan Wert [1,5], Bruce Henry[1], James R. Drummond[6], Gerd Hübler[3,4], and Tom Jobson[3,4]

Original Manuscript Date: December 2000

Published in
Journal of Geophysical Research
J. Geophys. Res. 107, 4039,
doi:10.1029/2000JD000260 (2002)

[1] NCAR, Boulder, Colorado
[2] Brookhaven National Lab, Upton, N.Y
[3] NOAA Aeronomy Lab, Boulder, Colorado
[4] Cooperative Institute for Research in Environmental Sciences, University of Colorado, Boulder, CO
[5] NCAR and the University of Colorado, Boulder, CO
[6] University of Toronto, Toronto, Canada

By acceptance of this article, the publisher and/or recipient acknowledges the U.S. Government's right to retain a nonexclusive, royalty-free license in and to any copyright covering this paper.

Research by BNL investigators was performed under the auspices of the U.S. Department of Energy under Contract No. DE-AC02-98CH10886.

Airborne CH_2O measurements over the North Atlantic during the 1997 NARE campaign: Instrument comparisons and distributions

Alan Fried,[1] Yin-Nan Lee,[2] Greg Frost,[3,4] Bryan Wert,[1,5] Bruce Henry,[1] James R. Drummond,[6] Gerd Hübler,[3,4] and Tom Jobson[3,4]

Received 14 December 2000; revised 24 May 2001; accepted 29 May 2001; published 28 February 2002.

[1] Airborne CH_2O measurements were acquired by tunable diode laser absorption spectroscopy (TDLAS) and coil/2,4-dinitrophenylhydrazine (CDNPH) techniques over remote regions of the North Atlantic Ocean from the surface to 8 km during the North Atlantic Regional Experiment (NARE-97) in September of 1997. There were eight aircraft flights when both instruments were simultaneously operating, producing 665 overlapping time intervals for comparisons. A number of approaches were used in the comparisons, and indicated that on average both instruments measured identical ambient CH_2O concentrations to within 0.1 ppbv, and more typically within 0.08 ppbv, over the 0 to 0.8 ppbv-concentration range. However, significant differences, larger than the combined 2σ total uncertainty estimates, were observed in 29% of the full time-coincident data set. The two instruments produced very similar altitude trends. Under clean background conditions in the 35° to 55°N latitude band, the median TDLAS and CDNPH CH_2O concentrations were 0.399 and 0.410 ppbv for 0–2 km, 0.250 and 0.355 ppbv for 2–4 km, and 0.217 and 0.280 ppbv for 4–8 km, respectively. Elevated CH_2O concentrations were observed in this study at both high altitudes (4–8 km) and in the marine boundary layer by both instruments. Thus vertical transport of CH_2O and/or its precursors may provide a greater contribution to upper tropospheric HO_x than previously thought. The results of this study, which are based upon instruments employing entirely different measurement principles, calibration, and sampling approaches, not only reinforce this conclusion but also provide a high-quality database necessary to further explore CH_2O measurement-model relationships in the clean background atmosphere. *Index Terms:* 0365 Atmospheric Composition and Structure: Troposphere—composition and chemistry; 0368 Atmospheric Composition and Structure: Troposphere—constituent transport and chemistry; 0394 Atmospheric Composition and Structure: Instruments and techniques; *Keywords:* formaldehyde, airborne measurements, tunable diode laser measurements, formaldehyde measurement comparisons, North Atlantic Regional Experiment measurements, airborne measurements of formaldehyde

1. Introduction

[2] Formaldehyde (CH_2O) is one of the most abundant gas phase carbonyl compounds found in the atmosphere. This relatively short-lived intermediate is formed by the oxidation of most anthropogenic and biogenic hydrocarbons initiated by reactions with the hydroxyl (OH) radical and ozone (O_3). In the continental planetary boundary, oxidation of nonmethane hydrocarbons (NMHCs) dominates the production of CH_2O. This gas is emitted directly by incomplete fossil fuel combustion as well as from secondary processes [*de Serves*, 1994; *Sigsby et al.*, 1987]. Formaldehyde is also emitted into the atmosphere from biomass burning [*Lee et al.*, 1997], industrial fugitive gas emissions, and emissions from vegetation [*Carlier et al.*, 1986, and references therein]. In the remote atmosphere, by contrast, methane (CH_4) oxidation becomes the dominant source of this gas.

[3] In addition to its reaction with OH (R1), CH_2O decomposes via two different photolysis channels, (R2a) and (R2b), which depend upon wavelength [*Calvert et al.*, 2000]:

$$\text{(R1)} \qquad CH_2O + OH \rightarrow HCO + H_2O$$

$$\text{(R2a)} \qquad CH_2O + h\nu(\lambda < 337\ \text{nm}) \rightarrow HCO + H$$

$$\text{(R2b)} \qquad CH_2 + h\nu(\lambda < 365\ \text{nm}) \rightarrow H_2 + CO.$$

In the lower atmosphere the radical products HCO and H generate the hydroperoxy radical HO_2 via

$$\text{(R3)} \qquad HCO_2 + O_2 \rightarrow HO_2 + CO$$

$$\text{(R4)} \qquad H + O_2 + M(N_2, O_2) \rightarrow HO_2 + M(N_2, O_2).$$

The radical photolysis channel (R2a) followed by (R3) and (R4) is a net source of odd hydrogen radicals, HO_x ($HO_x = HO_2 + OH + H$), in the atmosphere. This radical channel takes on greater importance during high solar zenith angles [*Fried et al.*, 1997b] and in the mid

[1]National Center for Atmospheric Research, Boulder, Colorado, USA.
[2] Brookhaven National Laboratory, Upton, New York, USA.
[3] Aeronomy Laboratory, NOAA, Boulder, Colorado, USA.
[4]Cooperative Institute for Research in Environmental Sciences, University of Colorado, Boulder, Colorado, USA.
[5]Department of Chemistry and Biochemistry, University of Colorado, Boulder, Colorado, USA.
[6] Department of Physics, University of Toronto, Toronto, Ontario, Canada.

Copyright 2002 by the American Geophysical Union.
0148-0227/02/2000JD000260$09.00

to upper troposphere where radical production from $O(^1D)$ with H_2O diminishes as the available H_2O vapor decreases with altitude [*Wennberg et al.*, 1998]. Finally, all three decomposition routes ultimately produce carbon monoxide (CO), and in air masses not influenced by local pollution these processes become a major source of CO to the global atmosphere [*McConnell et al.*, 1971].

[4] The chemistry of CH_2O is thus important in understanding the budgets and cycling among the odd hydrogen species OH and HO_2, odd nitrogen species NO and NO_2 (NO is converted to NO_2 in many steps which generate CH_2O), and the global budget of CO. Finally, as many hydrocarbon reactions initiated by OH or O_3 proceed through CH_2O as an intermediate, CH_2O becomes important in further testing our current understanding of hydrocarbon oxidation mechanisms in the troposphere.

[5] Because of the broad range of CH_2O sources, ambient measurements, carried out employing a wide variety of techniques, have exhibited high spatial and temporal variability. In urban areas, *Grosjean et al.* [1993] report ambient concentrations of 3 to 16 parts per billion by volume (ppbv) in many major cities. In more remote continental locations, ambient levels typically fall within the 1–2 ppbv range [*Harder et al.*, 1997; *Fried et al.*, 1997b; *Gilpin et al.*, 1997]. In the remote background atmosphere over the oceans, where the prevalence of continental CH_2O sources is minimized due to its short lifetime (typically several hours), ambient CH_2O concentrations are governed primarily by the immediate history of the air mass being sampled and ambient levels attain values that typically fall within the 0.1 to 0.5 ppbv range [*Neitzert and Seiler*, 1981; *Zafiriou et al.*, 1980; *Lowe and Schmidt*, 1983; *Harris et al.*, 1992; *Heikes*, 1992; *Heikes et al.*, 1996a; *Zhou et al.*, 1996; *Ayers et al.*, 1997]. Remote aircraft CH_2O measurements, which are far less extensive than those from the surface, yield ambient CH_2O concentrations ranging between approximately 0.04 and 1 ppbv, depending upon altitude and latitude. [*Arlander et al.*, 1995; *Jacob et al.*, 1996].

[6] In many of the studies cited above, ambient CH_2O observations were compared with theoretical model predictions. Such comparisons allow a simultaneous test of the current understanding of hydrocarbon photochemistry as well as the consistency with the OH concentrations employed. Under remote background conditions, where CH_4 oxidation is the primary CH_2O precursor, measurement-model comparisons have exhibited both positive and negative deviations. This divergence has raised numerous questions regarding both models and assumptions therein (including CH_2O sinks, photolysis frequencies, OH concentrations employed, and model CH_2O yields from CH_4 oxidation) as well as the veracity of the CH_2O measurements. Remote background measurements of CH_2O (median value of 105, parts per trillion by volume, pptv) during the first Mauna Loa Observatory study [*Heikes*, 1992] were found to be approximately a factor of 3 lower than box model results (300 pptv) calculated by *Liu et al.* [1992]. *Lowe and Schmidt* [1983] reported similar results. An extensive set of measurements, carried out during the second Mauna Loa Experiment (MLOPEX-II) employing five different techniques [*Heikes et al.*, 1996a], produced very similar free tropospheric background CH_2O concentrations to the first MLOPEX study; the two most extensive data sets produced ambient values between 100 and 150 pptv for all seasons [*Heikes et al.*, 1996a]. Although *Zhou et al.* [1996] showed qualitative agreement to within 14 to 75% between a simple photochemical model constrained by measurements of methylhydroperoxide (MHP, CH_3OOH) and their CH_2O data for MLOPEX-II, *Heikes et al.* [1996a] point out that other photochemical models at the Mauna Loa site or at comparable latitudes, altitudes, and seasons still yield unresolved measurement-model discrepancies by as much as a factor of 3. Comparisons by *Jacob et al.* [1996] during Transport and Atmospheric Chemistry Near the Equator-Atlantic (TRACE-A) indicated model overestimation by a factor of $\approx$4 in the 0–4 km range, which according to Jacob et al. implies a large missing CH_2O sink in the marine boundary layer or measurement errors. By contrast, the model underestimated the measurements in the middle troposphere (4–8 km) [*Jacob et al.*, 1996].

[7] *Arlander et al.* [1995] reported measured CH_2O concentrations more than a factor of 2 higher than those from a simple steady state calculation assuming CH_4 as the only CH_2O precursor. Likewise, *Ayers et al.* [1997] reported background CH_2O measurements (0.3 to 0.4 ppbv) that were almost a factor of 2 higher than their modeled values (0.2 ppbv). *Ayers et al.* [1997] raised the possibility that HO_2 radicals react with $CH_3O_2$to directly produce CH_2O without first going through MHP. During the Subsonic Assessment Ozone and Nitrogen Oxide Experiment (SONEX) airborne campaign over the North Atlantic in October–November of 1997, *Jaeglé et al.* [2000] obtained model results in the 8–12 km range that were systematically lower than the measurements by factors of 2 to 3 and did not capture the observed variability. These authors raise the possibility that heterogeneous conversion of methanol to CH_2O taking place on aerosols enhances the production of CH_2O.

[8] The above measurement-model discrepancies clearly point to considerable gaps in our understanding of CH_2O production, and possibly destruction pathways, in the clean background atmosphere and perhaps unresolved measurement issues as well. The present paper, in conjunction with the companion papers by *Wert et al.* [2002] and *Frost et al.* [2002], attempts to further address these issues with new airborne measurements and measurement-model comparisons of CH_2O in the remote marine background atmosphere. In this study, airborne CH_2O measurements were acquired over remote regions of the North Atlantic Ocean from the surface to 8 km during the 1997 North Atlantic Regional Experiment (NARE-97). Observations were acquired on board a National Oceanic and Atmospheric Administration (NOAA) WP-3 airplane in September of 1997 employing two independent techniques, tunable diode laser absorption spectroscopy (TDLAS) and coil/2,4-dinitrophenylhydrazine (CDNPH). These techniques are based upon different measurement principles, calibration, and sampling approaches. Earlier versions of both instruments were employed in a ground-based intercomparison study and produced agreement to within 11% for ambient concentrations in the 1–5 ppbv range, and to within 4% when the results were normalized to a common set of calibration standards [*Gilpin et al.*, 1997]. This agreement coupled with numerous laboratory inlet tests carried out by *Wert et al.* [2002], standards verification, and comparison measurements adds considerable confidence to the present airborne CH_2O measurement data set. The combined measurements presented here thus provide a high-quality database necessary to further explore CH_2O measurement-model relationships in the clean remote background atmosphere.

2. Aircraft CH_2O Instruments

[9] The TDLAS and CDNPH systems were developed and operated by personnel at the National Center for Atmospheric Research (NCAR) and the Brookhaven National Laboratory (BNL), respectively. Since both instruments have been described in detail elsewhere (TDLAS system [*Fried et al.*, 1997a, 1998a, 1998b, 1999; *Gilpin et al.*, 1997; *Wert et al.*, 1996] and CDNPH system [*Lee et al.*, 1996; *Gilpin et al.*, 1997]), the present paper will only briefly discuss each instrument. However, details particularly pertinent to the NARE-97 mission and measurement accuracy will be highlighted and/or reemphasized in the present paper.

2.1. Tunable Diode Laser Absorption Spectrometer

[10] The IR radiation from a liquid-nitrogen-cooled lead-salt diode laser was directed through a multipass astigmatic Herriott cell (Aerodyne Research Inc.) and on to indium-antimonide photovoltaic detectors. The IR beam, which traces out a Lissajous pattern in the cell, achieves a total optical path length of 100 m in only a 3-

L sampling volume. Data were acquired using second harmonic detection coupled with sweep integration, as further discussed by *Fried et al.* [1998a]. More comprehensive details of the TDLAS system are given by the authors cited above.

[11] The inlet, as further discussed by *Wert et al.* [2002], is composed of a rear-facing heated 1-inch OD glass-lined stainless steel tube, which continuously passed ambient air through the Herriott cell at flow rates around 8 standard liters per minute (sLpm, where standard conditions are defined as 273 K and 760 torr). A flow control valve at the cell entrance maintained cell pressures around 25 torr. Zero air, generated by employing a second inlet using a diaphragm pump and a heated Pd/Al_2O_3 scrubber, was used to acquire background spectra. This scrubbing system very effectively removes CH_2O without significantly affecting the ambient water vapor concentration. During background acquisition the zero airflow was rerouted and reintroduced back into the inlet at flow rates exceeding the sample flow. As discussed by *Fried et al.* [1998a, 1998b], background spectra were acquired approximately twice every minute, and this approach very effectively captures and removes optical noise as well as the effects of sample line outgassing. In the companion paper by *Wert et al.* [2002], extensive laboratory tests of this inlet were carried out under temperature, pressure, and relative humidity conditions representative of those encountered during airborne operation.

[12] For calibration purposes, standards were generated using a CH_2O permeation system, the output of which was periodically added to the main inlet line. The calibration system contained two different permeation devices with different emission rates housed in separate glass chambers in a temperature-controlled (68.9° ± 0.2°C) aluminum block. The CH_2O emissions rates were determined before and after the NARE-97 mission by comparisons with gas standards from a laboratory Henry's law calibration system (HLCS). The HLCS output was determined employing the temperature-dependent Henry's law coefficients of *Dong and Dasgupta* [1986] together with measurements of solution concentration, Henry's law saturation flow, and pressure. The calculated HLCS output has been verified by direct absorption spectroscopy, by two different cartridge methods, and by additional permeation devices calibrated by gravimetry [*Fried et al.*, 1997a; *Gilpin et al.*, 1997]. On the basis of all the collective calibrations we estimate a total calibration uncertainty of ±6% at the 1σ level for both permeation devices. During the 1997 NARE mission the CDNPH instrument sampled both CH_2O permeation standards while the airplane was on the ground. Employing aqueous CH_2O standards, the CDNPH instrument retrieved an average CH_2O concentration that was 8.2 ± 5.9% different from the input values for the two permeation devices and a median difference of 4.5%. Further details regarding the inlet, calibration, and zeroing systems are given by *Fried et al.* [1998b, 1999] and *Wert et al.* [2002].

[13] At the flows employed, CH_2O standards in the 10–12 ppbv range were typically generated at the cell entrance. Since the calibration system was not pressure-controlled, the permeation devices were exposed to varying pressures as the aircraft altitude changed. In-flight calibrations as well as subsequent laboratory tests definitively showed that the effective permeation output increased by as much as 30% at altitudes around 8 km. This effect, which we believe is associated with a change in the instantaneous wall conditioning of the permeating devices, was no longer present at pressure altitudes less than 2 km. Therefore ambient TDLAS data for each flight were refit using one or two low-altitude (*P*alt < 2 km) flight calibrations acquired on that flight. The flight calibrations chosen for this purpose produced instrument sensitivities within 3.9 ± 2.5% of other low-altitude calibrations acquired during the mission as well as laboratory values acquired using similar cell pressures, temperatures, modulation waveform, and modulation amplitudes. Continuously measuring and normalizing each ambient measurement to laser power eliminates the effect of potential alignment changes. Calibration changes due to cell pressure and temperature changes should not be present since both are continuously controlled and/or measured. Cell pressures around 25 torr were controlled on any given flight to within ±2 torr. Although these changes are relatively small, an empirical calibration matrix based on laboratory data was developed and applied to the fitting procedure to account for such pressure changes. This procedure was further verified using a theoretical approach. The companion paper by *Wert et al.* [2002] further shows no significant changes in the inlet line transmission efficiency with changes in sampling pressure, temperature, and relative humidity. Thus employing selected low-altitude flight calibrations should not produce measurement errors larger than a few percent at most.

[14] During airborne operation, TDLAS measurements of CH_2O were acquired by averaging an ambient sample for 20 s. Background spectra were acquired for 10 s before and after each ambient sample using an appropriate delay period of 6 s (approximately 5 inlet/cell *e*-folding times) after each switch. The backgrounds surrounding each ambient were averaged and subtracted point by point from the ambient spectrum. Each background-subtracted ambient spectrum was fit in real time to a background-subtracted calibration spectrum acquired previously employing a multiple linear regression approach [*Sewell et al.*, 1993]. Typically, the ambient-flush-background acquisition sequence was repeated for 20–30 min before a new calibration spectrum was acquired. After every third calibration, three additional calibration runs (designated pseudoambients) were sequentially acquired and processed exactly the same as an ambient spectrum. This procedure helped to ensure data quality by (1) identifying potentially bad individual calibrations; (2) identifying potential errors in the data acquisition/fitting retrieval procedures; and (3) providing a direct measure of instrument precision. Each entire ambient acquisition cycle, which included the acquisition of two backgrounds and one ambient spectrum, delay periods, and computer-processing overhead, took approximately 1 min. Henceforth we will refer to each ambient acquisition cycle so acquired as a 1-min average.

[15] In all cases, TDLAS measurements were carried out employing an isolated CH_2O absorption feature at 2831.6417 cm^{-1}. The nearest interfering absorption line listed in the HITRAN database [*Rothman et al.*, 1996] is from O_3 and is 0.0787 cm^{-1} lower in frequency and over 5 orders of magnitude weaker in strength. The nearest H_2O line is 0.1993 cm^{-1} away, and at sampling pressures around 25 torr, *Fried et al.* [1998a] have shown that H_2O vapor mixing ratios as high as 2% do not have an effect on retrieved CH_2O mixing ratios as low as 100 pptv. Spectral interferences from various organic molecules, including methanol, ethanol, 2-propanol, acetaldehyde, propanal, butanal, 2-methylpropanal, acetone, isoprene, methylethylketone, and a mixture of C_2 to C_{16} alkanes, were further tested. Of these, the only minor problem was from methanol (CH_3OH); for every 1 ppbv of CH_2O, 1 ppbv of CH_3OH resulted in 0.039 ppbv higher retrieved CH_2O values. Ambient CH_3OH concentrations in the remote marine atmosphere typically fall within the 50 to 800 pptv range [*Singh et al.*, 1995; *Jaeglé et al.*, 2000]. The latter was measured during the SONEX mission over the same region only 1 to 2 months later. Thus CH_3OH should produce a maximum interference of only +31 pptv in our ambient CH_2O values, and more typically around +15 pptv for remote background CH_3OH concentrations around 400 pptv. However, since no actual CH_3OH concentrations were measured during NARE-97, no corrections were applied to the present TDLAS measurements of CH_2O.

2.2. Coil/2,4-Dinitrophenylhydrazine (CDNPH) Instrument

[16] *Lee and Zhou* [1993] discuss the CDNPH technique applied to ambient measurements of CH_2O, and *Lee et al.* [1996, 1998] further discuss the batch wise configuration deployed on the WP3 aircraft during the 1997 NARE campaign. Ambient measurements

Table 1. Tunable Diode Laser Absorption Spectroscopy (TDLAS) and Coil/2,4-Dinitrophenylhydrazine (CDNPH) Measurement Precision and Systematic Uncertainty Estimates (at 1σ Level) for Each Flight as a Function of GPS Altitude[a]

Date/ Altitude, km	TDLAS 1-min Precision	TDLAS 5-min Precision	TDLAS Systematic Uncertainty, %	CDNPH 5-min Precision	CDNPH Systematic Uncertainty, %	Combined Precision (1σ)
Sept. 13, 1997	0.119	0.067	7.5			
0–2				0.060	13.5	0.090
2–4				0.068	15.0	0.095
4–8				0.079	18.0	0.104
Sept. 16, 1997	0.087	0.049	7.5			
0–2				0.060	13.5	0.077
2–4				0.068	15.0	0.084
4–8				0.079	18.0	0.093
Sept. 18, 1997	0.085	0.048	7.2			
0–2				0.060	13.5	0.077
2–4				0.068	15.0	0.083
4–8				0.079	18.0	0.092
Sept. 20, 1997	0.100	0.057	7.3			
0–2				0.060	13.5	0.083
2–4				0.068	15.0	0.089
4–8				0.079	18.0	0.097
Sept. 22, 1997	0.110	0.062	7.3			
0–2				0.040	9.0	0.074
2–4				0.045	10.0	0.077
4–8				0.053	12.0	0.082
Sept. 24, 1997	0.101	0.057	7.3			
0–2				0.040	9.0	0.070
2–4				0.045	10.0	0.073
4–8				0.053	12.0	0.079
Sept. 26, 1997	0.098	0.056	7.2			
0–2				0.040	9.0	0.069
2–4				0.045	10.0	0.072
4–8				0.053	12.0	0.077
Sept. 29, 1997	0.099	0.056	7.2			
0–2				0.040	9.0	0.069
2–4				0.045	10.0	0.072
4–8				0.053	12.0	0.077

[a] The 1-min and 5-min TDLAS results are averages of ambient data over 20 and 100 s, respectively (see text). All precision estimates are in ppbv, and the systematic terms are percent of ambient. The combined measurement precision estimate for both instruments (at 1σ level) was derived by quadrature addition of the individual 5-min instrument precision terms.

were acquired using the following steps: (1) sampling ambient formaldehyde by incorporating the gas into an aqueous solution containing the DNPH derivatizing reagent using a 28-turn glass coil, (2) storing the liquid samples sequentially in septum-sealed glass vials using an autosampler, and (3) analyzing the dissolved formaldehyde as the DNPH derivative on the ground after the flight using a high-performance liquid chromatograph (HPLC) equipped with a UV-Visible detector. We give below an overview of the basics and operation of the CDNPH-HPLC technique used on the WP3. For additional details the reader is referred to the publications listed above.

[17] Ambient air was drawn through the inlet, a section of 1/4-inch OD PFA Teflon tubing ~110 cm long. Approximately 50 cm of this tubing protruded outside the aircraft and was enclosed in a rear-facing metal housing. Similar to the TDLAS system [see *Wert et al.,* 2002], the sampling line was shielded by an inverted stainless steel funnel to prevent liquid water droplets accreted on the metal housing during passages in clouds from entering the sample inlet. The 1/4-inch Teflon sample line was connected to a 28-turn Pyrex coil scrubber mounted inside the aircraft. Sample air was drawn through this scrubber at 2.0 sLpm by an air pump and controlled by a mass flow controller (MKS, 0–5 sLpm). An aqueous solution containing 0.10 m*M* DNPH with the pH maintained at 2.50 using H_2SO_4 was pumped by a peristaltic pump to the head of the coil at a flow rate of 0.30 mL min^{-1}. This solution mixed with the sample air and scrubbed the gaseous formaldehyde. At the end of the coil scrubber the liquid was separated from the air and was pumped by the same peristaltic pump to an autosampler (ISCO, model ISIS) for storage in glass vials (volume ~2.0 mL) sealed with a Teflon-coated silicone septum. The autosampler was programmed to fill each vial for 5.0 min, which represented the time resolution of this formaldehyde technique as well as the period over which the samples were integrated.

[18] Analyzing the samples typically began within 2 hours after landing. To prepare for the analysis, blanks and formaldehyde standards were prepared with the very DNPH scrubbing solution used for the flight, which was freshly prepared before each flight. The formaldehyde standards were prepared from successive dilution of a 10.0 m*M* standard, which in turn was prepared from a 37% solution, and the concentrations of the working standards ranged from 0.25 to 1.0 μ*M*. In order to determine the liquid flow rate each sample vial was weighed using an analytical balance before and after sampling. The difference in weight is the amount of liquid collected and hence the liquid flow rate.

[19] The samples were analyzed using an automated HPLC system, which consisted of an autosampler (Gilson, Model 234XL), an HPLC pump (Hitachi, Model 6200A), a C18 reverse phase column (Microsorb-MV, 3 μm, Rainin Instruments), a UV-Visible detector (Spectra-Physics, Model UV-2000), and a computer-controlled interface (Rainin, Model Dynamax) that controls the HPLC analysis and stores the resulting chromatograms. The analysis was performed using isocratic elution (60% H_2O: 40% CH_3OH) and a monitor wavelength of 370 nm; samples were analyzed sequentially every 5.0 min, and the injection volume was 0.50 mL. Typically, 110–120 samples were collected on each flight and, together with the additional 12 blanks and standards, took 10 hours for the analysis to finish.

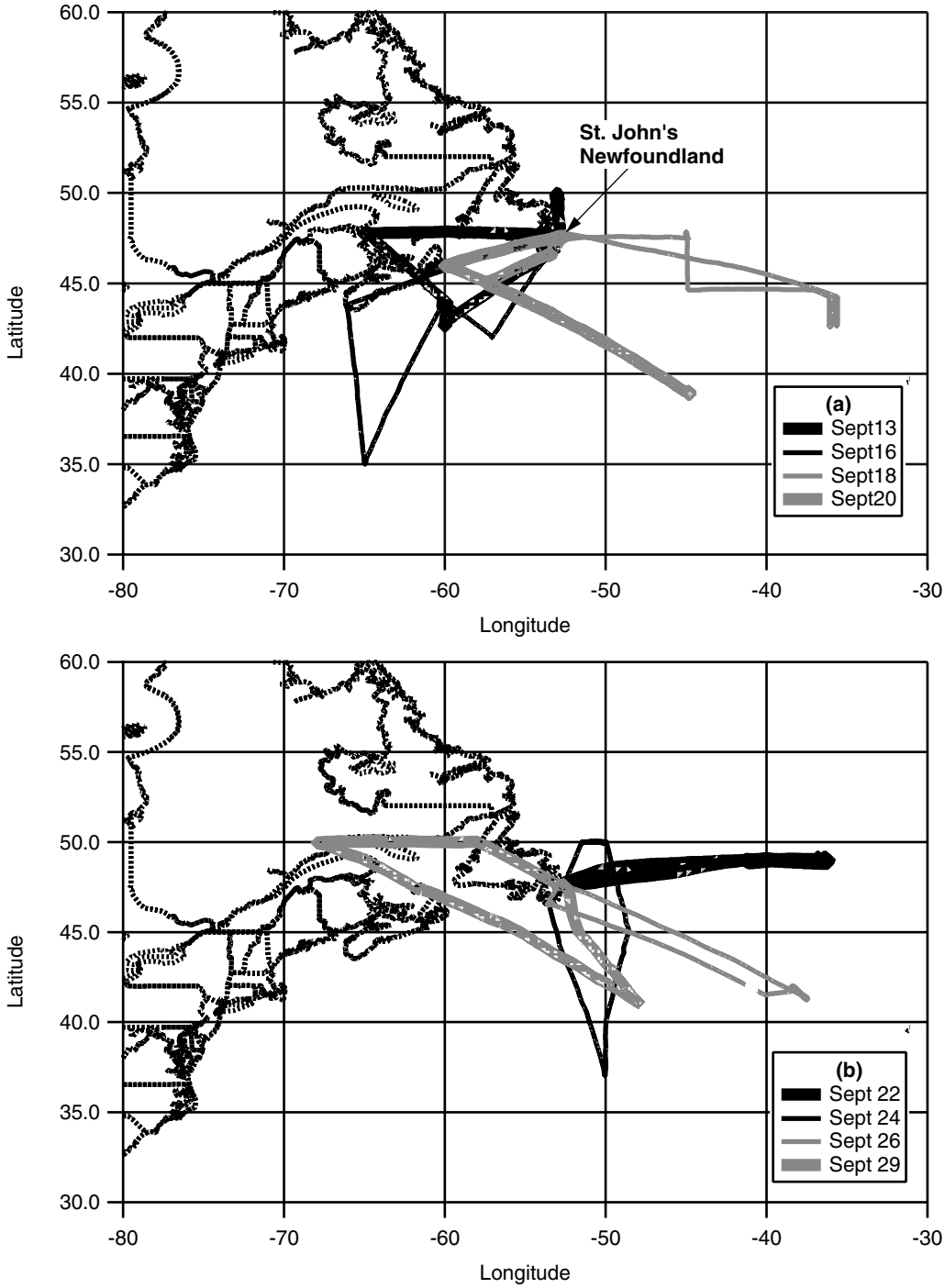

Figure 1. Flight tracks for the eight different NARE flights (September 13–29, 1997) when both instruments were fully operational and recording ambient CH_2O measurements for comparison purposes.

[20] The formaldehyde collection efficiency of the coil scrubber is less than 100% because formaldehyde has a limited Henry's law solubility ($6 \times 10^3 M$ atm^{-1} at 22°C). The collection efficiency of the 28-turn coil was determined in the laboratory using a walk-in altitude chamber under a range of conditions, namely, gas flow rate (2–4 sLpm), liquid flow rate (0.2–0.4 mL min^{-1}), and atmospheric pressure (0.4–1.0 atm), and the results have been reported elsewhere [*Lee et al.*, 1996]. The collection efficiency was found to be insensitive to temperature between 0° and 30°C [*Lee and Zhou*, 1993], but varies as a function of pressure [*Lee et al.*, 1996] as well as the gas and liquid flow rates. At a gas flow rate of 2.0 ± 0.1 sLpm and a liquid flow of 0.30 ± 0.1 mL min^{-1}, the collection efficiency is 0.72 at 1 atm pressure and decreases with decreasing pressure until 0.63 atm when the collection efficiency stabilizes at 0.49 [*Lee et al.*, 1996].

3. Measurement Precision and Accuracy Estimates

[21] As discussed by *Fried et al.* [1998a], the true measure of TDLAS instrument precision is obtained from the standard devia-

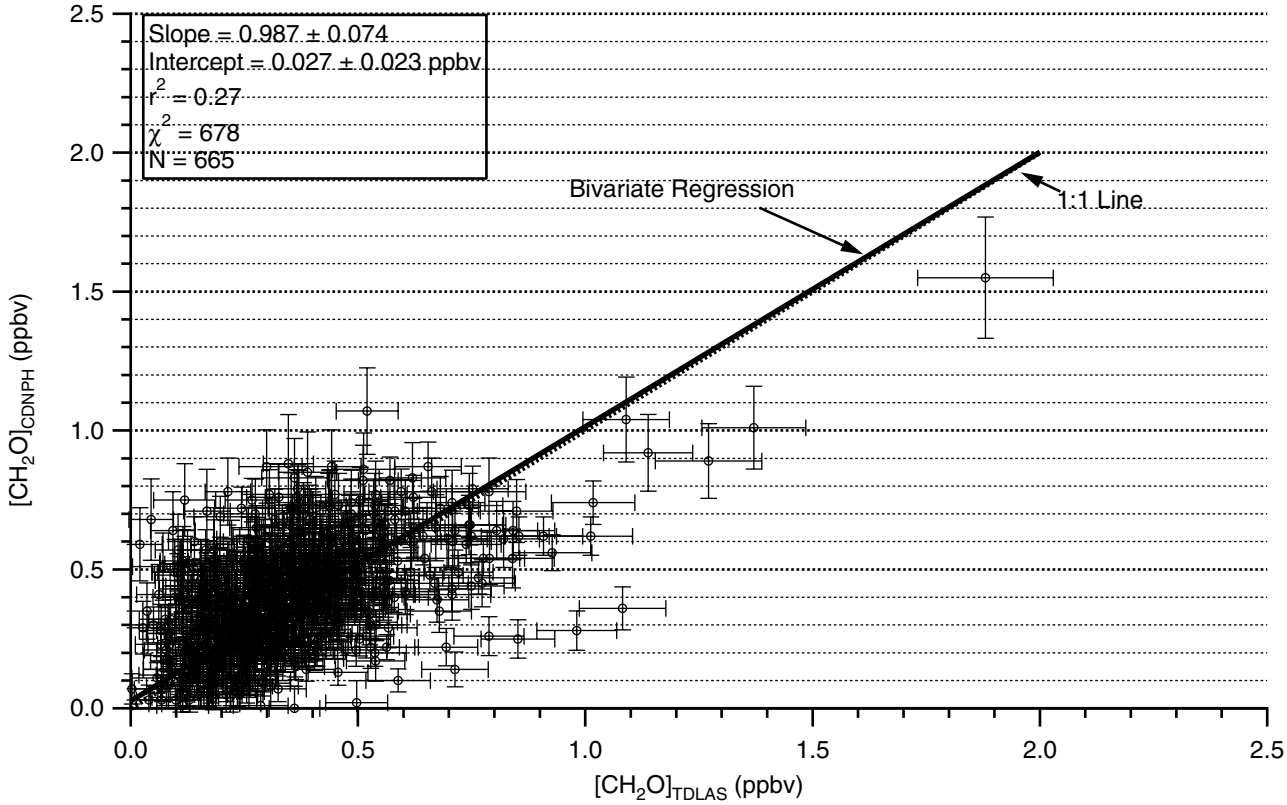

Figure 2. Scatterplot for the time-coincident 5-min measurements from both instruments for the eight different flights along with a weighted bivariate linear regression fit (solid line) and the 1:1 line (dashed line).

tion of replicate measurements (σ_r) upon sampling a constant input. The periodically acquired pseudoambient calibrations provided such a direct determination in some cases. Most of the time, the TDLAS precision was based upon the precision of adjacent background differences, which surround each ambient (σ_{Bkg}) spectrum. As discussed by *Wert et al.* [1996] and *Fried et al.* [1998a], this approach approximates an upper limit to the true instrument precision; based upon laboratory standards as well as constant ambient CH_2O samples in the 0–5 ppbv range, *Fried et al.* [1998a] have determined a ratio σ_{Bkg}/σ_r of 1.4 ± 0.4. Table 1 lists the 1-min TDLAS ambient measurement precision estimates (1σ level) averaged over each flight obtained from σ_{Bkg} and from σ_r of pseudoambient measurements where possible. In a subsequent section these on-line TDLAS precision estimates will be further compared with those obtained from the ambient measurement precision upon sampling a constant air mass. As can be seen in Table 1, the 1-min sampling sequence produced an estimated TDLAS precision that ranged between 0.085 and 0.119 ppbv and averaged 0.100 ppbv. As the present optical system was not temperature-stabilized, the precision was primarily limited by subtle time-dependent alignment changes, which in turn produced small changes in the background structure between ambient and background acquisition cycles. At sampling pressures around 25 torr, temperatures around 298 K, and a 100-m path length, an average measurement precision of 0.100 ppbv corresponds to a line center absorbance of 2.9×10^{-6}. Following the NARE-97 mission, the entire optical system, including the optical bench, was mounted in a temperature-controlled enclosure. This, along with numerous other improvements discussed by *Wert et al.* [1999], now routinely yield 1σ airborne CH_2O measurement precisions of 0.030–0.035 ppbv for 1 min of averaging.

[22] For comparison purposes with the CDNPH measurements each 1-min TDLAS ambient sampling cycle was further averaged over the CDNPH sampling interval using a trapezoidal routine, resulting in 665 overlapping 5-min time-coincident intervals. Since the sampling intervals between the two instruments did not perfectly match and at times there were missing data, the "5-min" TDLAS sample on average was composed of 4.3 measurements. On the basis of the precision improvement with time from *Fried et al.* [1998a], the 1-min TDLAS precision estimates should improve to 0.048–0.079 ppbv when averaging over the 5-min CDNPH interval. These estimates are given in the third column of Table 1 for each flight. The estimated TDLAS systematic uncertainty (1σ level) ranges between 7.2 and 7.5% for each flight (fourth column of Table 1), and was determined by quadrature addition of the various measurement uncertainties. A total measurement uncertainty was then calculated for every TDLAS measurement by quadrature addition of the measurement precision with the systematic estimate (systematic uncertainty × measured concentration).

[23] Table 1 also lists the 5-min CDNPH measurement precision for each flight in three different altitude bins (0–2, 2–4, and 4–8 km) as determined from the baseline precision of the HPLC analysis. At the 1σ level these estimates range between 0.040 and 0.079 ppbv. The systematic uncertainty was derived by quadrature addition of various terms which reflect the altitude-dependent uncertainty in the following: the coil scrubber efficiency (≈6 to 8%), sample airflow rate (≈2 to 5%), liquid flow rate (≈2 to 3%), chromatographic integration (≈3%), injection volume (≈3%), span calibration (≈5%), and liquid standards preparation (≈2%). This analysis results in a total systematic uncertainty of 9–18% for the three different altitude bins (sixth column of Table 1). Because of instrument problems encountered during the ground analysis, the systematic uncertainty for measurements on September 13, 16, 18, and 20 flights were 50% higher than other flights. As with the TDLAS, a total CDNPH measurement uncertainty (1σ) was determined for every data point by quadrature addition of the measurement precision with the systematic estimate. Improve-

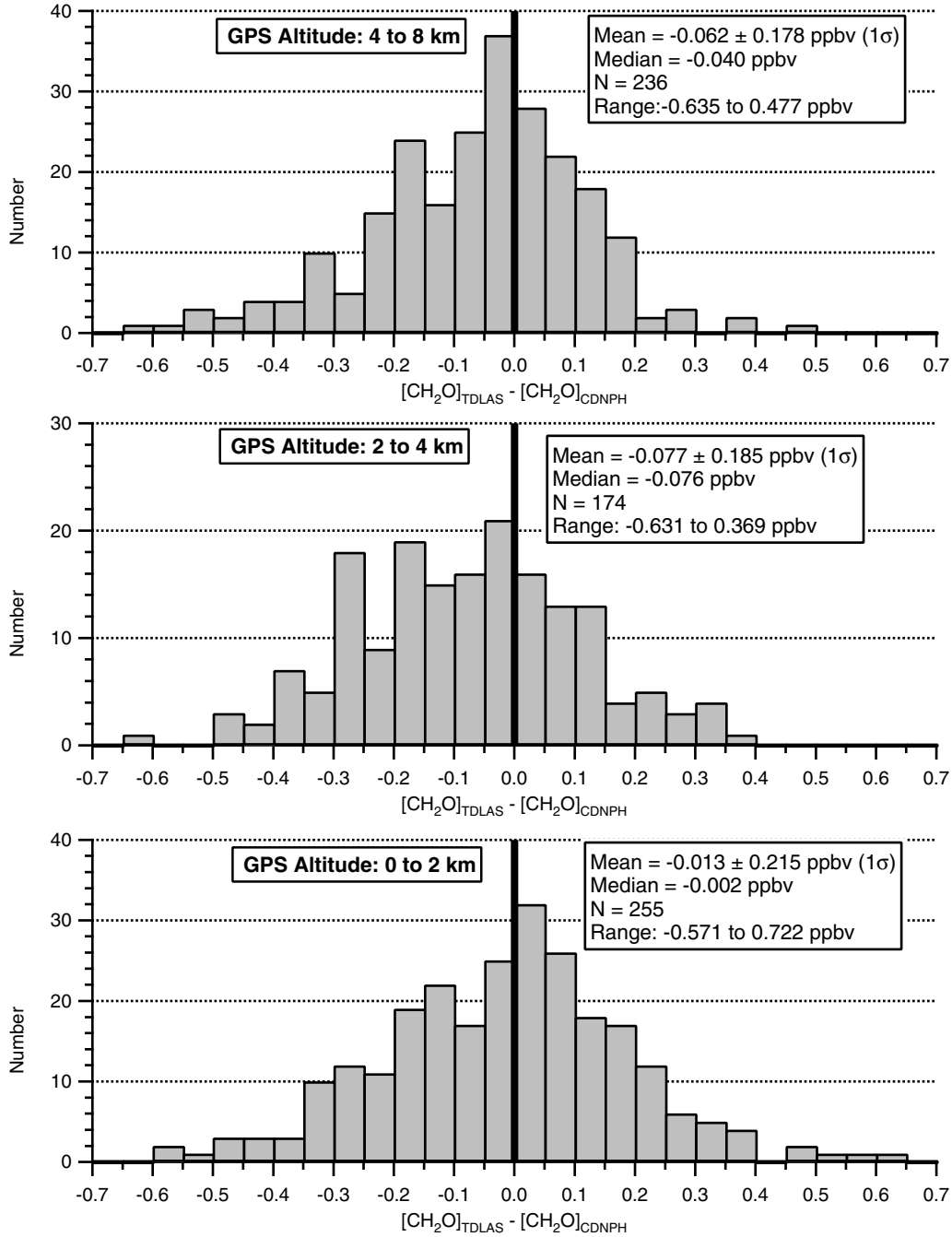

Figure 3. Histograms (0.05 ppbv-bin size) of the measurement difference ($[CH_2O]_{TDLAS}$ - $[CH_2O]_{CDNPH}$) in ppbv for three different altitude ranges.

ments to the CDNPH system since the NARE mission yield similar precisions as Table 1 but with an improved time resolution of 2 min.

[24] As shown in Table 1, the measurement precision and total uncertainty estimates from both instruments are very comparable. The seventh column of Table 1 lists the combined measurement precision ("5 min") of the two techniques at the 1σ level, obtained by quadrature addition of the individual instrument precision estimates. A combined total uncertainty estimate was also calculated for the two techniques by quadrature addition of the individual instrument total uncertainty estimates. These combined estimates, which assume independent, normally distributed measurements, as well as random systematic components, give an overall range within which one should expect measurements from the two instruments to agree. This will be further discussed in a subsequent section.

4. Aircraft Campaign and Intercomparison Protocol

[25] The NARE mission took place throughout September 1997 and was based out of St. Johns, Newfoundland, Canada. The resulting flight tracks traversed an area bounded by −74° to −36° longitude, and 35°N to 55°N latitude. These flights, which sampled at altitudes ranging between 0.05 and 8 km, were

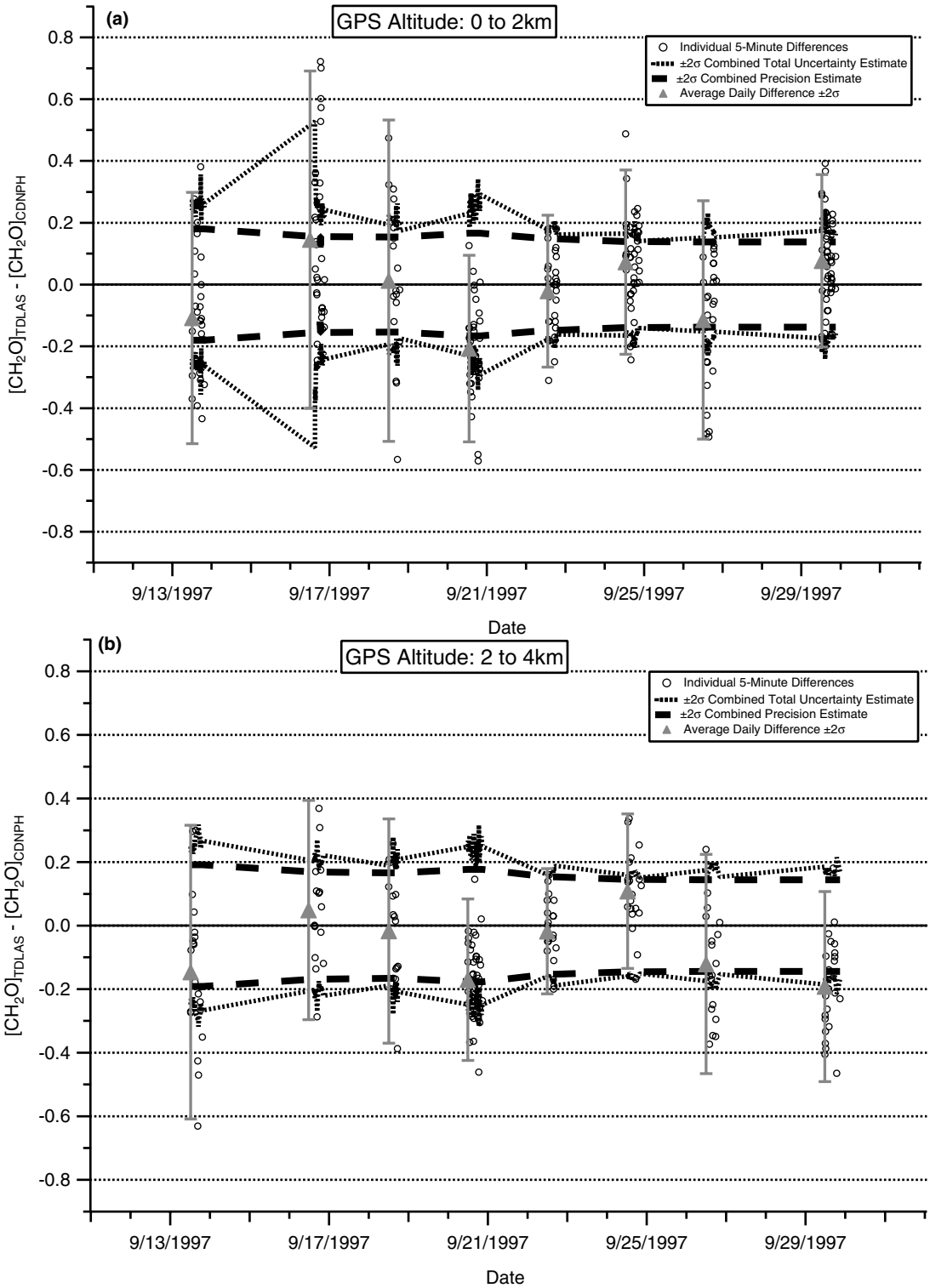

Figure 4. Individual measurement differences for each flight in three altitude ranges in units of ppbv. The open circles display the individual 5-min differences, while the average daily differences and the ±2σ spread in these daily means are denoted by the large solid triangles and associated error bars, respectively. Also displayed are the combined precision estimates (dark dashed lines) and combined total uncertainty estimates (dark dotted lines) at the 2σ level derived from the data of Table 1.

primarily over the North Atlantic Ocean. Figure 1 displays flight tracks for the eight different NARE flights (September 13–29, 1997) when both instruments were fully operational and recording ambient CH_2O measurements. The flight locations were designed to sample synoptic midlatitude storms arising from cold-frontal passage from the North American continent. As discussed by *Bethan et al.* [1998], these frontal systems can readily redistribute boundary layer air vertically, and occurred

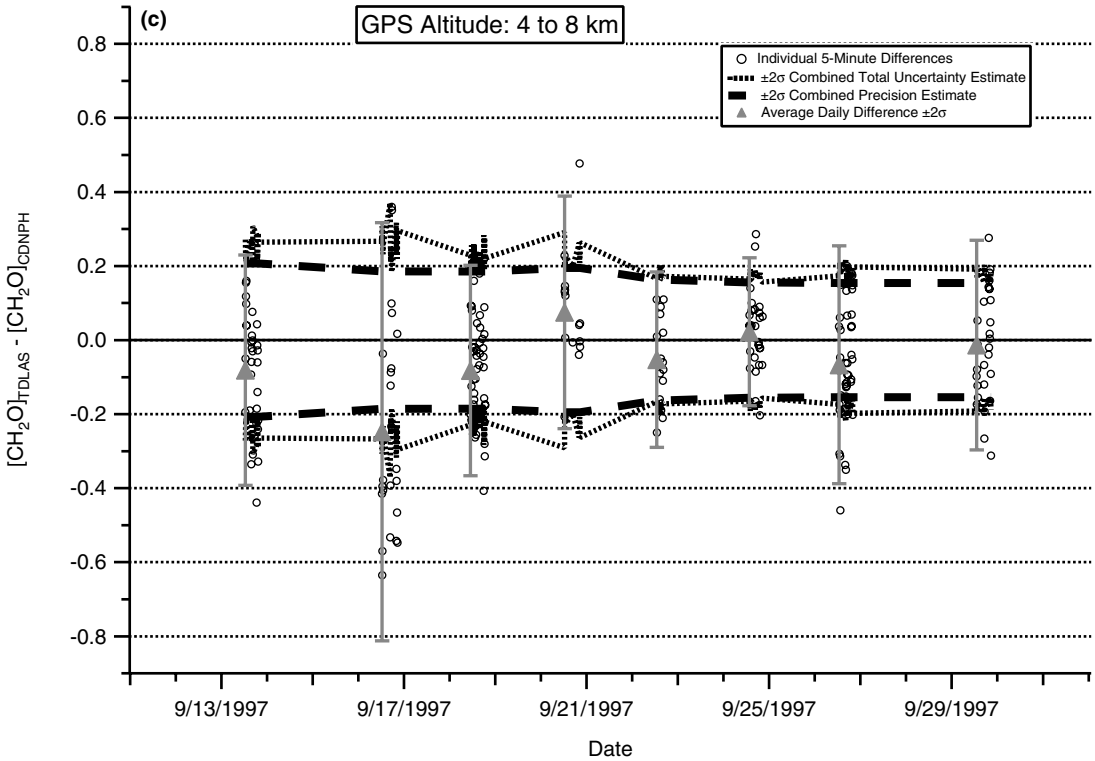

Figure 4. (continued).

with a frequency approximately every 5 days. Throughout the campaign, the daily results were fully available to all participants, and at no time was the comparison rigorously blind. However, rigorous final data were analyzed and subsequently submitted by both groups independently to NOAA personnel without any further communications.

5. CH_2O Measurement Comparisons

[26] Following the lead of *Harder et al.* [1997], a number of approaches were used to compare the ambient CH_2O measurements from the two instruments.

5.1. Comparison Using Bivariate Linear Regression

[27] Figure 2 displays a scatterplot for the time-coincident 5-min measurements along with the 1σ total uncertainty estimates. A weighted bivariate linear regression, using the procedure developed by *Neri et al.* [1989], is also shown. This procedure minimizes the sum of the squared perpendicular distances between each experimental point and the regression line. Each data point was weighted by the square of the reciprocal of the total uncertainty. As can be seen, the regression and 1:1 lines are nearly equivalent; one obtains identical slopes within the 1σ standard error limit indicated in the inset. However, this regression analysis does not yield the complete picture, especially since there is relatively large scatter about the regression line (r^2 = 0.27). Although much of the scatter reflects the close proximity to the detection limits of both instruments, there are a number of points in Figure 2 at ambient concentrations greater than 0.5 ppbv where discrepancies as large as a factor 3 are evident. All of these points occur at altitudes less than 2 km, and may reflect a shortcoming in calculating time-coincident data in the presence of high and variable ambient CH_2O levels; the "5-min" TDLAS data were obtained by averaging five distinct 20-s ambient acquisitions, while the CDNPH measurements reflect a true 5-min ambient integration. Thus it is highly likely that the two instruments may be effectively capturing different ambient samples.

5.2. Comparison Using Histograms of the Measurement Differences

[28] The 5-min time-coincident measurements were used to generate measurement difference ($[CH_2O]_{TDLAS}$ - $[CH_2O]_{CDNPH}$) histograms as a function of altitude. Figure 3 displays histograms (0.05 ppbv-bin size) and associated statistics for three different altitude ranges (0–2, 2–4, and 4–8 km). Although the CDNPH results are slightly larger than the TDLAS measurements for all three bins, both instruments on average yield the same CH_2O concentrations: the mean and median differences fall within the 0.002–0.077 ppbv range. Despite the fact that the distribution spread and data range is largest in the 0–2 km altitude range, the mean and median differences are smallest for this altitude range. This suggests that although individual comparison points may reflect the aforementioned sampling issue, on average the instrument agreement does not show any definitive concentration dependence. This will be further discussed in a later section.

[29] The spread in the distributions of Figure 3 in all cases is higher than the combined measurement precisions of Table 1 by a factor of 2 to 3. Although the aforementioned sampling issue might explain some of the increased spread at lower altitudes, these observations suggest that one or both instruments on average is less precise than anticipated and/or variable systematic errors may be present at times. This same result was observed during the ground-based study of *Gilpin et al.* [1997] when sampling constant ambient CH_2O levels around 2 ppbv.

5.3. Comparisons of Measurement Differences as a Function of Flight, Altitude, and Concentration

[30] Figures 4a–4c display the measurement differences for each flight in the three altitude ranges along with the combined precision and total uncertainty estimates (2σ level) derived from

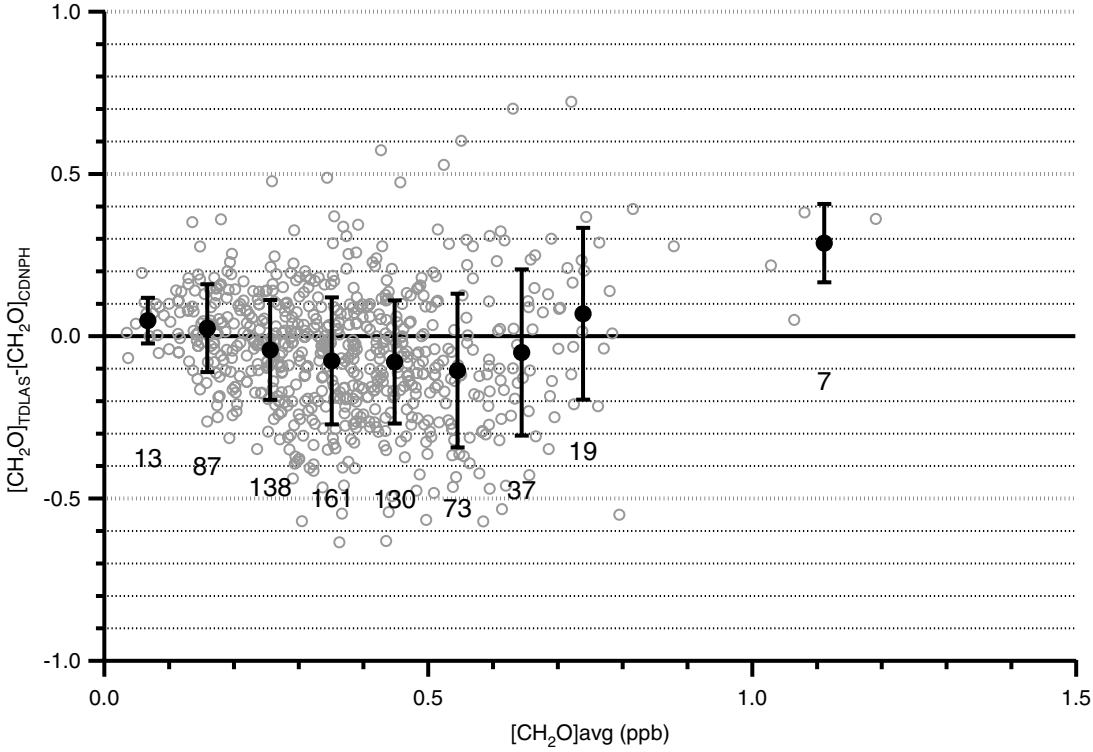

Figure 5. Plot of the measurement difference (TDLAS - CDNPH) in ppbv for all the 665 time-coincident results (open circles) as a function of the average CH_2O concentration recorded by both instruments. The larger dark points denote the average measurement difference calculated for each 0.1 ppbv measurement interval. The associated error bars represent the 1σ spread in the measurement difference for each interval, and the numbers beneath each determination denote the number of measurements in each interval.

Table 1. The combined precision estimates in most cases comprise most of the total uncertainty. In all cases the average daily differences fall within the combined total uncertainty limits. However, as in Figure 3, the individual 5-min measurement differences as well as the spread in the average daily differences (error bars on the triangle points) show additional sources of uncertainty. In all but a few cases the spread in the average daily differences are larger than the combined total estimated uncertainty limits. In the 0–2 km range, 69% of the individual 5-min differences fall within the ±2σ combined total uncertainty limits. This is very similar to the results for the 2–4 km (67%) and 4–8 km (77%) altitude ranges. For all three altitude ranges combined, 71% of the individual 5-min differences fall within the ±2σ combined total uncertainty limits. One would expect that 95% of the measurements should fall within these limits in a normally distributed data set. In Figure 4a, measurements on September 16 and 18, 1997, display the largest spreads in the average daily differences. In Figures 4b and 4c, data acquired on September 13 and 16, 1997, respectively, show likewise extraordinarily large spreads. In addition, the average daily differences for data acquired on September 20, 1997, in Figure 4a, September 29, 1997, in Figure 4b, and September 16, 1997, in Figure 4c are very close to the lower 2σ combined total uncertainty limit. It is therefore useful to further investigate the measurement differences for these time periods as a function of other measured parameters. This is particularly true for data acquired on September 16, 1997, in Figure 4c, where both the average daily difference and associated spread falls within the above categories. In addition, the spread in the measurement difference for these data is the largest of the entire mission.

[31] We examined the measurement differences as a function of numerous variables, including positive and negative altitude changes, ambient dew point, relative humidity, and ambient CH_2O levels. No unequivocal correlations were observed. Since the inlets for the two instruments were sufficiently different (TDLAS inlet is heated, zeroed, and back-flushed with zero air before takeoff, while none of the above procedures were adopted for the CDNPH inlet), we further examined the ambient levels of various gases, including NO, NO_y, CO, H_2O mixing ratio as well as relative humidity, and liquid water, prior to takeoff. This is an attempt to identify time periods when inlet contamination could explain the observed airborne comparisons. We present this in light of the results observed in the companion study by *Wert et al.* [2002] where CH_2O desorption from the walls of a nonheated Teflon inlet was sometimes observed under conditions where high ambient CH_2O levels were sampled and where it was likely that liquid H_2O may have collected. On September 16, 1997, the highest H_2O (9.8 g kg^{-1}), NO, and NO_y concentrations (both exceeded 300 ppbv) were measured on board the WP3 aircraft prior to takeoff. Although speculative at this point, it is possible that the large deviations observed at the start of this flight (mean $[CH_2O]_{TDLAS} - [CH_2O]_{CDNPH} = -0.405$ ppbv for seven contiguous measurements) as well as other flights might be associated with CH_2O desorption from the CDNPH inlet after takeoff.

[32] The lack of any obvious concentration dependence is further shown in Figure 5. In this plot the measurement differences (TDLAS - CDNPH) for all the 665 time-coincident results are displayed as a function of the average CH_2O concentration recorded by both instruments. The larger solid points denote the average measurement difference calculated for each 0.1 ppbv measurement interval, and the associated error bars represent the 1σ spread in the measurement difference for each interval. At ambient CH_2O concentrations ranging between 0 and 0.8 ppbv the average difference for each interval of Figure 5 does not show a clear concentration dependence; the average measurement difference starts out at +0.048 ppbv, attains a maximum value of −0.106 ppbv in the 0.5–0.6 ppbv bin, and rises back

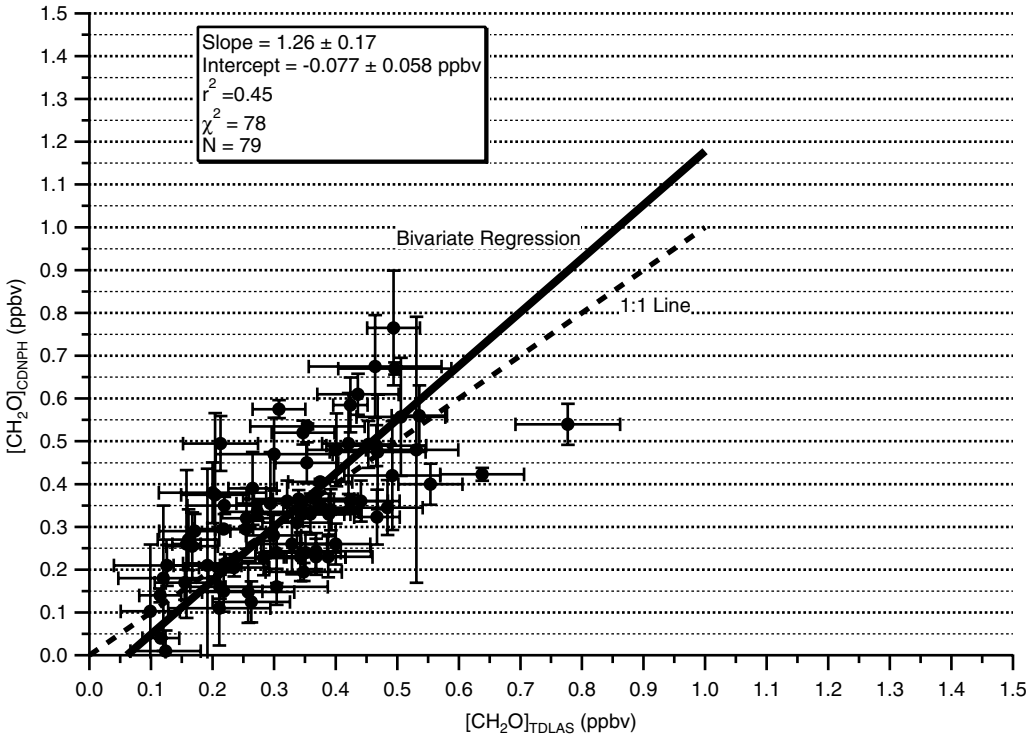

Figure 6. Bivariate regression plot of the CDNPH data versus the TDLAS using a subset of 79 points based on constant air mass legs.

up to +0.069 ppbv in the 0.7–0.8 ppbv bin. In all cases the spread in each bin spans the zero difference line.

[33] Thus, at CH_2O levels between 0 and 0.8 ppbv, Figure 5 yields a consistent picture with all previous plots; namely, on average there is no systematic difference between airborne CH_2O measurements from the two instruments. At concentrations greater than 0.8 ppbv the seven time-coincident measurements suggest a systematic difference of +0.287 ± 0.121 ppbv between the two measurements. However, this is based on a limited number of data points that span the concentration range between 0.8 and 1.7 ppbv.

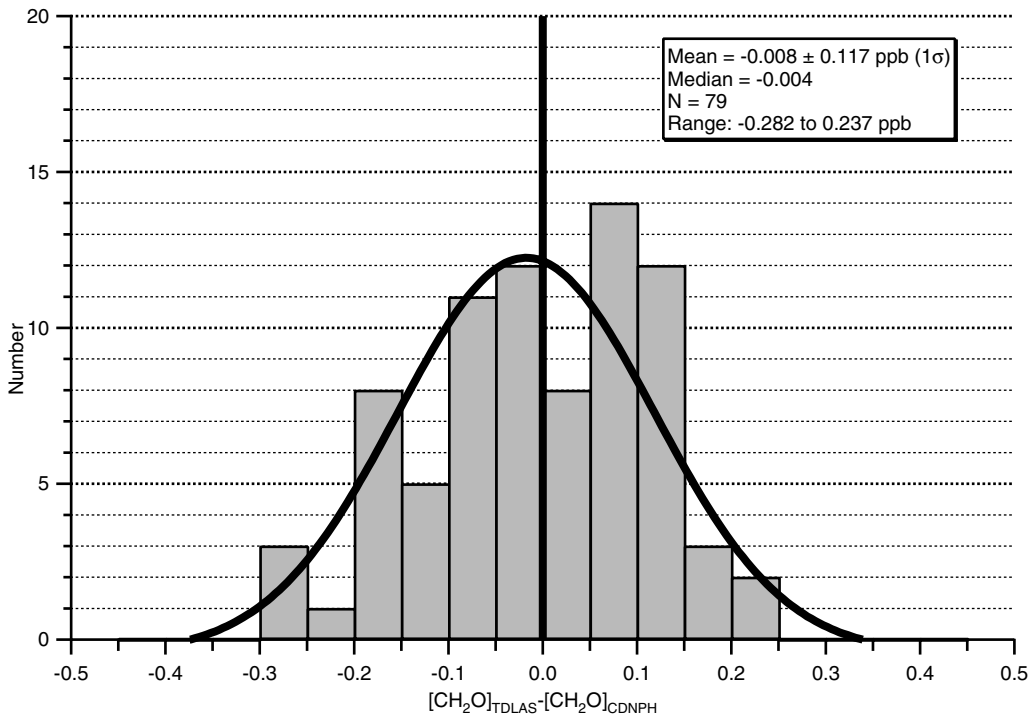

Figure 7. Histogram (0.05 ppbv-bin size) of the measurement difference in ppbv for the reduced 79-point constant air mass data set. The dark curve denotes a Gaussian fit.

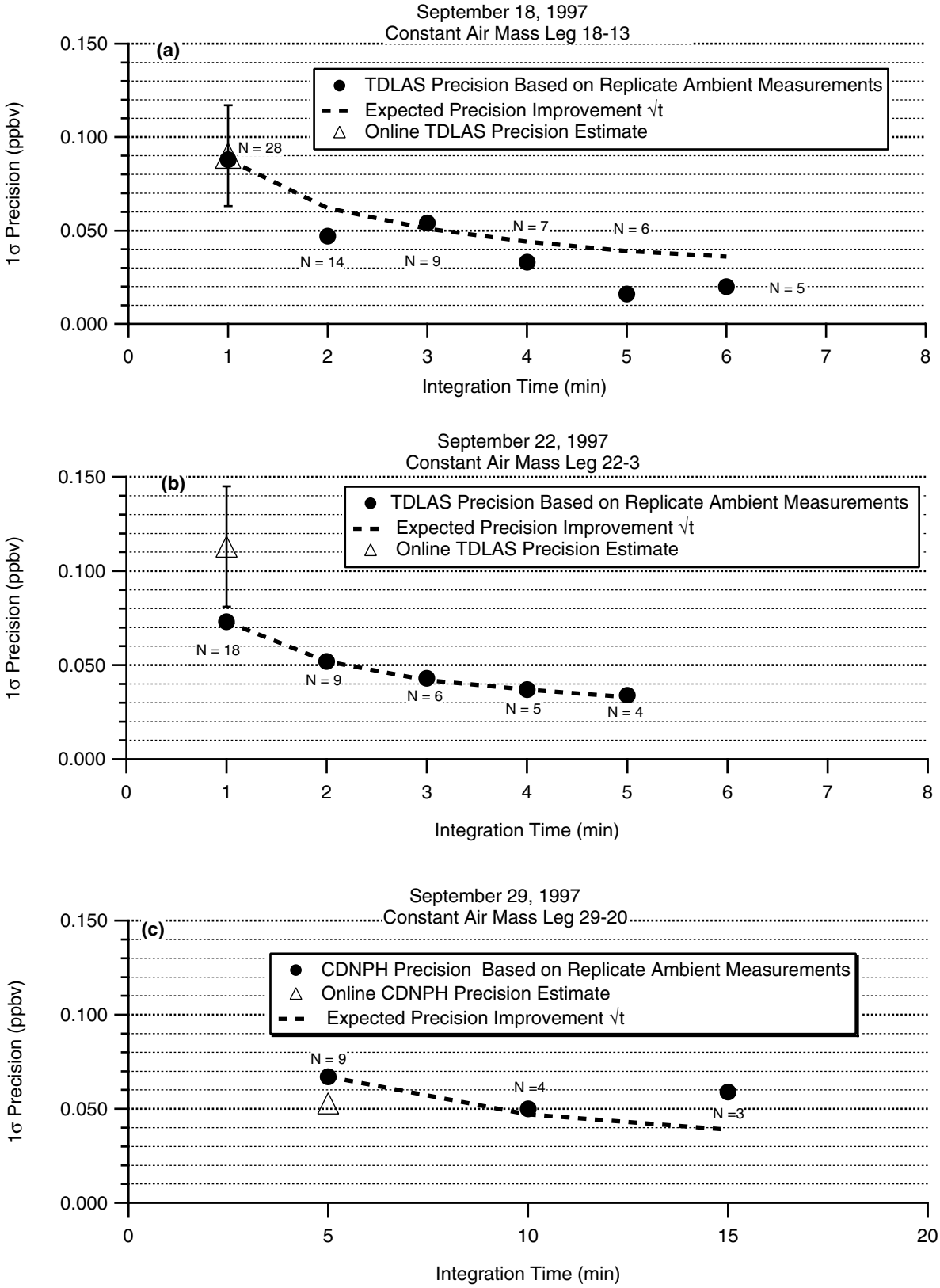

Figure 8. (a) Ambient 1-min TDLAS measurements acquired during a 33-min long constant air mass leg on September 18 along with various precision determinations, as further discussed in the text. (b) Same format as Figure 8a for 1-min TDLAS data acquired on September 22. (c) Same analysis for a 50-min long leg with the CDNPH instrument on September 29.

Table 2. Best Measurement Precisions for One or Both Instruments Based on the Replicate Ambient Measurements During the Constant Air Mass Legs[a]

GPS Altitude, km	$[CH_2O]_{TDLAS}$	$1\sigma_{TDLAS}$	$[CH_2O]_{CDNPH}$	$1\sigma_{CDNPH}$
3.1	0.283	0.064	0.227	0.040
4.6	0.167	0.042	0.255	0.079
4.4	0.155	0.049	0.170	0.040
4.6	0.158	0.023	0.260	0.173
3.1	0.424	0.028	0.585	0.064
3.1	0.453	0.037	0.493	0.055
0.5	0.494	0.043		
3.0	0.212	0.048	0.160	0.028
3.1	0.115	0.034	0.140	0.016
0.6	0.421	0.043	0.495	0.118
5.7	0.265	0.039		
5.7	0.116	0.030		
0.5	0.340	0.090	0.365	0.021
5.0	0.255	0.042	0.320	0.071
0.4	0.367	0.069	0.365	0.017
7.6	0.251	0.065	0.176	0.067

[a] The measured concentrations, which represent the mean values during the leg, and 1σ-precisions, are in ppbv. The precisions are for 5 min of averaging. Missing CDNPH data reflect shorter averaging legs where the number of points is less than 3.

The comparisons for these points may also reflect the aforementioned sampling issue.

5.4. Constant Air Mass Legs and Measurement Comparisons

[34] One can gain further insight into the instrument comparisons by parsing the measured CH_2O data into time periods when the air mass being sampled is constant. Such constant air mass legs minimize measurement discrepancies arising from the strictly nonoverlapping sampling times between the two instruments, and allow one to average over time periods longer than 5-min to improve the instrument measurement precisions. Such improved precision in turn makes it possible to identify systematic differences in the instruments. As discussed in the companion paper by *Frost et al.* [2002], identification of constant air mass legs further provides a timebase for averaging inputs into a box model for CH_2O measurement-model comparisons. In cases where the constant air mass leg is composed of a sufficiently large number of ambient samples, the standard deviation of the ambient measurements provides a direct determination of the measurement precision, and hence a cross-check on the precision estimates of Table 1 as well as the identification of favorable cases where the measurement precision is both low and unequivocal for optimal measurement-model comparisons.

[35] Constant air mass legs (N = 177) were identified by the constancy in a number of air mass tracers, including altitude, equivalent potential temperature, and relative humidity. The standard deviations in equivalent potential temperature and relative humidity were required to be less than 1 K and 7%, respectively. The total change in altitude throughout most such legs was between 100 and 1200 m. Although slightly different criteria can be chosen, all the air parcels encountered within a constant air mass leg were homogeneous and had similar back trajectories, which were obtained from the Cambridge Trajectory Server (M. J. Evans, http://www.atm.ch.cam.ac.uk/~mathew/trajectories/start.html,

Table 3. Tunable Diode Laser Absorption Spectroscopy (TDLAS) and Coil/2,4-Dinitrophenylhydrazine (CDNPH) Time-Coincident 5-min CH_2O Distributions as a Function of GPS Altitude for the 35°–55°N Latitude Range[a]

Measurement	Altitude Bin, km	Mean	Median	Range	N	Air Mass Type
TDLAS	0–2	0.490 ± 0.217	0.446	0.076–1.880	225	I
CDNPH		0.503 ± 0.203	0.490	0.080–1.550		
TDLAS	0–2	0.405 ± 0.144	0.399	0.076–0.776	84	II
CDNPH		0.428 ± 0.176	0.410	0.080–0.870		
TDLAS	0–2	0.538 ± 0.236	0.485	0.112–1.880	170	III
CDNPH		0.548 ± 0.204	0.560	0.100–1.550		
TDLAS	2–4	0.312 ± 0.131	0.300	0.070–0.840	174	I
CDNPH		0.389 ± 0.175	0.400	0.040–0.850		
TDLAS	2–4	0.251 ± 0.096	0.250	0.078–0.511	78	II
CDNPH		0.365 ± 0.155	0.355	0.090–0.770		
TDLAS	2–4	0.367 ± 0.134	0.364	0.070–0.840	94	III
CDNPH		0.410 ± 0.187	0.415	0.050–0.850		
TDLAS	4–8	0.234 ± 0.109	0.224	0.003–0.533	236	I
CDNPH		0.296 ± 0.160	0.290	−0.040–0.880		
TDLAS	4–8	0.218 ± 0.105	0.217	0.003–0.503	123	II
CDNPH		0.287 ± 0.164	0.280	−0.040–0.710		
TDLAS	4–8	0.252 ± 0.109	0.246	0.027–0.533	113	III
CDNPH		0.308 ± 0.159	0.290	−0.040–0.880		

[a] All concentrations and 1σ standard deviations (given with the mean values) are in ppbv. Three air mass types are presented: (I) where all the time-coincident measurements are given (a total of 665 for the three altitude bins); (II) time-coincident measurements for clean background conditions where [CO] < 95 ppbv, [NO] < 20 pptv, $[NO_y]$ < 500 pptv, and $[C_2Cl_4]$ < 5 pptv; and (III) time-coincident measurements where the air mass shows evidence of anthropogenic inputs, in this case any one of the conditions in type II are not met. In some cases the number of measurements (N) for the parsed air masses (II and III) do not add up to the total (air mass I) since some of the parsing tracers are missing.

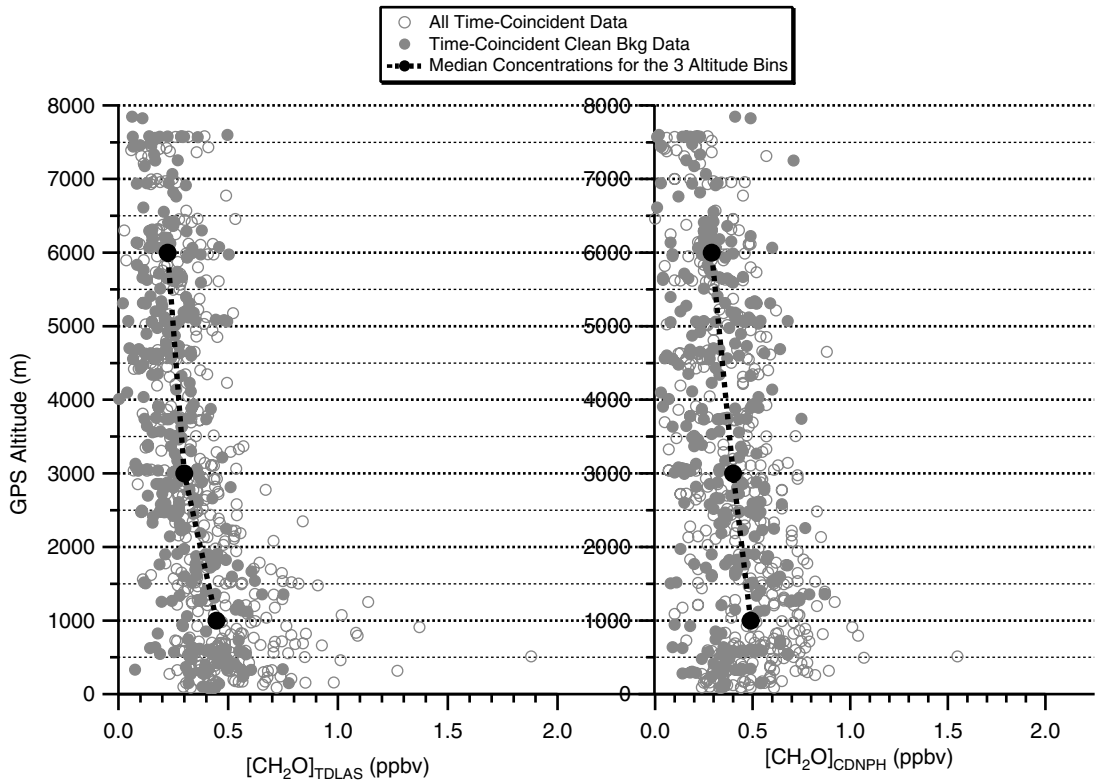

Figure 9. Altitude plot of the 665 time-coincident 5-min CH_2O measurements from both instruments.

1999); in 95% of the cases the air encountered during a given constant air mass leg had a similar origin both vertically and horizontally within 2 days. As discussed by *Frost et al.* [2002], the constancy in chemical tracers such as O_3, CO, and NO_y was further used to parse the data set to 87 constant air mass legs. These legs ranged in duration between 7 and 51 min long.

[36] Figures 6 and 7 reproduce the bivariate regression and difference histogram plot of Figures 2 and 3, respectively, using the reduced data set from the constant air mass legs. An additional eight points were eliminated in this analysis to eliminate points potentially influenced by the possible inlet effects previously discussed, resulting in a final data set of 79 comparison points. As can be seen in Figure 6, the regression line has a steeper slope and larger negative intercept than that of Figure 2. This is reasonable given that the full data set of Figure 2 contains a number of very low points relative to the regression line that significantly reduce the slope and raise the intercept. These points are not included in the regression of Figure 6. Although the instrument agreement in Figure 6 appears to be worse than Figure 2, the correlation coefficient is nearly double that of Figure 2. On the basis of the results of Figure 6 the difference between the regression-calculated and input CH_2O concentrations averages −0.038 ppbv over the 0 to 0.8 ppbv-concentration range.

[37] Figure 7, which displays a histogram of the measurement difference for the reduced 79-point data set, gives nearly identical information. A Gaussian fit is also included to indicate a normal distribution. As shown, the measurement differences are nearly normally distributed, and the mean and median differences are very close to zero. In addition, the 1σ standard deviation of the measurement difference is 0.117 ppbv, which is considerably smaller than values for the full data set (see Figure 3). Furthermore, the 0.117 ppbv distribution spread is not too different from the combined estimated precision of Table 1, the average value of which is 0.081 ± 0.010 ppbv. Lastly, only 3 of the 79 data points (3.8%) lie outside the combined 2σ total uncertainty limits, in agreement with that expected for a Gaussian distribution. Thus the reduced 79-point constant air mass data set eliminates much of the extra variability observed in the full 665-point comparison data set.

5.5. Constant Air Mass Legs and Measurement Precision

[38] The extra variability in the full 665 time-coincident data set invariably reflects over optimism in the precision estimates of Table 1 and/or periodic unknown experimental problems in one or both instruments. Fortunately, the constant air mass legs, especially those composed of a large number of ambient samples, provide a direct determination of the actual measurement precisions to cross-check the estimates of Table 1. This is particularly true for the TDLAS data where the 1-min ambient measurements provide the needed data density for an accurate precision determination and an assessment of how this precision improves with averaging time. The assumption here is that the criteria used in selecting the constant air mass legs are sufficiently robust to guarantee constant ambient CH_2O levels. Thus any measurement variability is solely attributable to the instrument.

[39] The plots of Figure 8 show how this analysis is used. In Figure 8a, ambient 1-min TDLAS measurements were acquired during a 33-min long constant air mass leg on September 18. The estimated on-line precision yields a value of 0.090 ppbv, and this is denoted in the figure by the open triangle and its associated error estimate. The replicate precision of the 28 one-minute ambient measurements spanning this constant air mass leg was determined from the ambient measurement standard deviation. The value of 0.088 ppbv, denoted by the solid circle, is in very close agreement with the on-line precision estimate. The ambient replicate precision was then determined for longer TDLAS measurement averages by binning the 1-min TDLAS data into successively longer averages. The solid circles show how the measurement improves with averaging time; the dashed-line denotes a simple square root time dependence. As some of the integration times are not integer divisors of the starting number of points, some of the intervals for the higher averaging

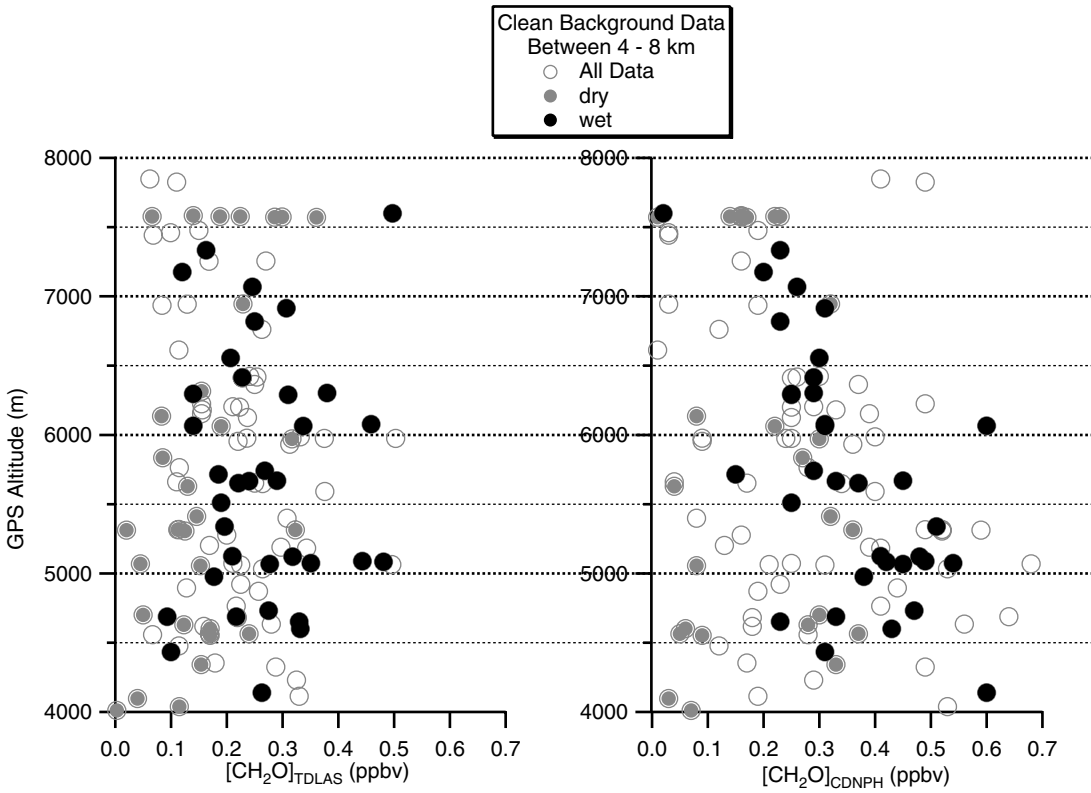

Figure 10. Display of all the time-coincident clean background measurements (Type II) from both instruments (open points) in the upper altitude bin between 4 and 8 km. The data are further parsed into wet and dry air mass types (see text and Table 4).

times had to use the same points in more than one interval. The TDLAS measurement precision for averaging time periods between 4 and 6 min falls within the 0.016 to 0.033 ppbv range. In this particular case the actual measurement precision appears to improve faster than the square root time dependence. Figure 8b displays a 19-min long TDLAS measurement leg where the measurement precision improves with a square root time dependence. The 1-min on-line precision estimate in this case is larger than the ambient replicate precision (0.113 compared to 0.073 ppbv). At 5-min of averaging, a measurement precision of 0.034 ppbv is obtained. Figure 8c shows the same analysis for a 50 min long leg with the CDNPH instrument. Unfortunately, this is the only leg long enough to show how the 5-min CDNPH measurement precision improves with time. As with Figure 8a, the CDNPH ambient replicate precision (0.067 ppbv) is close to the on-line precision estimate of 0.053 ppbv. The precision attains a value of 0.050 ppbv after 10 min of averaging.

[40] Sixty-nine percent of the 1-min TDLAS data yield replicate precision measurements during the constant air mass legs that are either nearly equivalent to or are smaller than the on-line precision estimates of Table 1. In the other 31%, where the replicate measurements are higher than the on-line precision estimates, the median value for the discrepancy is 0.060 ppbv and falls within the range 0.032–0.234 ppbv. Unfortunately, only about 25% of the 5-min CDNPH measurements had enough points (at least three) during the constant air mass legs to determine accurately the ambient replicate precision. Fourteen percent of the CDNPH replicate measurements were found to be higher than the on-line precision estimates of Table 1. The

Table 4. Clean Background Tunable Diode Laser Absorption Spectroscopy (TDLAS) and Coil/2,4-Dinitrophenylhydrazine (CDNPH) Time-Coincident 5-min CH_2O Distributions for the 4–8 km Altitude Bin Parsed for Wet and Dry Air Masses[a]

	TDLAS Wet	CDNPH Wet	TDLAS Dry	CDNPH Dry
Mean	0.266	0.350	0.157	0.178
s.d.	0.104	0.129	0.091	0.122
Median	0.257	0.310	0.150	0.165
N	36	35	32	26
Maximum	0.497	0.600	0.361	0.370
Minimum	0.093	0.020	0.003	−0.040

[a] Units are in ppbv. The air mass was considered wet if the measured H_2O mixing ratio in g kg^{-1} was greater than the mean measured mixing ratio, determined for each 0.5 km bin for the NARE campaign, plus 1 standard deviation. Likewise, dry air masses were selected where the measured H_2O mixing ratio was less than the measured mean minus 1 standard deviation.

Table 5. One-Minute Tunable Diode Laser Absorption Spectroscopy (TDLAS) CH_2O Distributions as a Function of GPS Altitude for the Entire NARE Campaign[a]

Altitude Bin, km	Mean	Median	Range	*N*	Air Mass Type
0–2	0.560 ± 0.460	0.465	−0.064–4.493	1304	I
0–2	0.398 ± 0.188	0.387	−0.064–0.953	297	II
0–2	0.608 ± 0.504	0.494	−0.004–4.493	1007	III
2–4	0.312 ± 0.177	0.299	−0.058–0.962	894	I
2–4	0.242 ± 0.155	0.217	−0.057–0.962	280	II
2–4	0.344 ± 0.178	0.342	−0.058–0.945	614	III
4–8	0.227 ± 0.145	0.214	−0.096–0.882	1098	I
4–8	0.216 ± 0.138	0.206	−0.089–0.666	382	II
4–8	0.233 ± 0.149	0.217	−0.096–0.882	716	III

[a] In addition to the faster time response (compared to the 5-min data of Table 3), these measurements also include an additional flight (the October 2, 1997, transit flight from St. Johns to Tampa, Florida) not in Table 3. All concentrations and 1σ standard deviations (given with the mean values) are in ppbv. Three air mass types are presented: (I) where all the measurements are given (a total of 3296 for the three altitude bins); (II) measurements for clean background conditions where [CO] < 95 ppbv, [NO] < 20 pptv, $[NO_y]$ < 500 pptv, and $[C_2Cl_4]$ < 5 pptv; and (III) measurements where the air mass shows evidence of anthropogenic inputs, in this case any one of the conditions in type II are not met. In some cases the number of measurements (*N*) for the parsed air masses (II and III) do not add up to the total (air mass I) since some of the parsing tracers are missing.

median value and range for this discrepancy are 0.078 ppbv and 0.077–0.094 ppbv, respectively. Because of the limited number of CDNPH replicate precision determinations, one cannot make a relative comparison between the total number of TDLAS and CDNPH measurements that exhibit precisions greater than those estimated in Table 1. Nevertheless, this analysis suggests that a nontrivial number of measurements for the complete 665-point data set from both instruments may be less precise than those indicated in Table 1. This is in agreement with Figures 3 and 4, where 29% of the 665 comparison data points fall outside the combined total estimated 2σ measurement uncertainties.

[41] In Table 2 we tabulate the best measurement precisions for both instruments based on the replicate ambient measurements during the constant air mass legs. In most cases, the precisions improved in a predictable way similar to those of Figure 8. A bivariate regression of the 13 data points in Table 2 yields a slope of 1.27 and an intercept of −0.040 with an r^2 of 0.79. Since the slope and intercept are nearly identical to those of Figure 6, this suggests that the less precise but broader 79-point data set of Figure 6 accurately reflects the relationship between the two instruments. In addition, these particularly favorable air mass legs represent interesting cases that will be further compared to box model calculations in the companion paper by *Frost et al.* [2002].

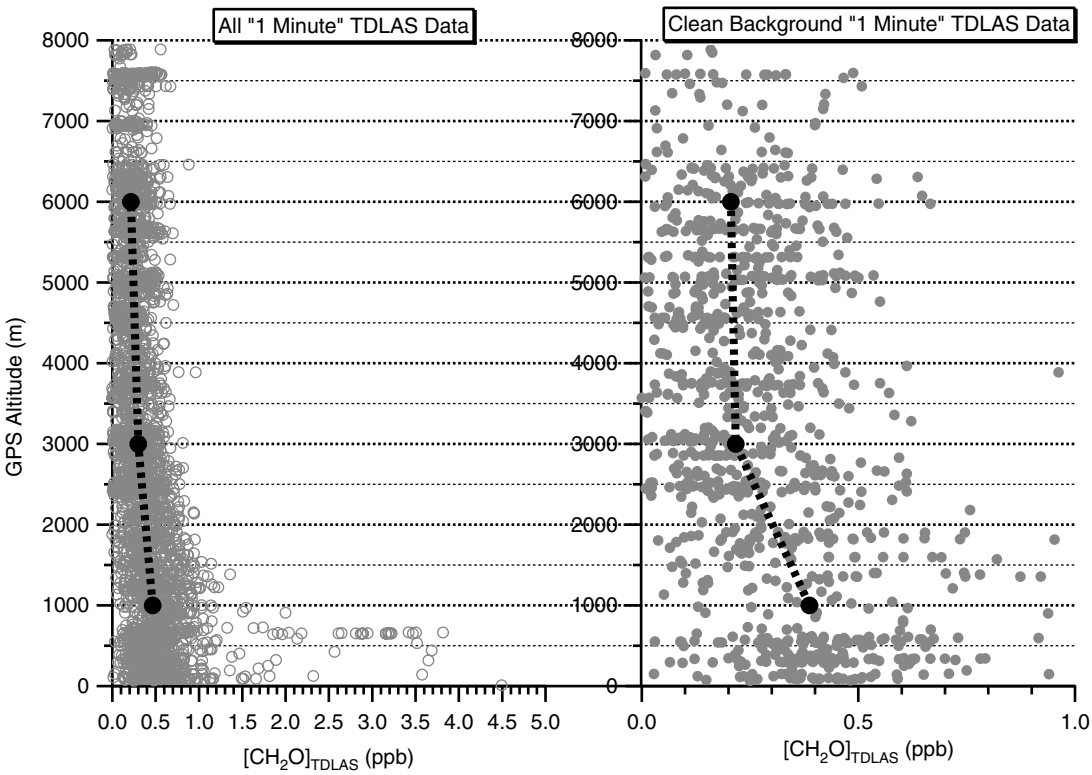

Figure 11. Altitude plot for all the 1-min TDLAS measurements (open circles in left panel) acquired during the NARE campaign and the clean background measurements (solid circles in right panel). The large dark circles denote the median concentrations measured for the three altitude bins.

Table 6. Analog of Table 4, With 1-min TDLAS Measurements[a]

	TDLAS Wet	TDLAS Dry
Mean	0.256	0.159
s.d.	0.149	0.115
Median	0.254	0.136
N	99	98
Maximum	0.647	0.464
Minimum	−0.082	−0.089

[a] All CH_2O distributions (in ppbv) represent clean background conditions for the 4–8 km altitude bin parsed for wet and dry air masses. The air mass was considered wet if the measured H_2O mixing ratio in g kg^{-1} was greater than the mean measured mixing ratio, determined for each 0.5 km bin, plus 1 standard deviation. Likewise, dry air masses were selected where the measured H_2O mixing ratio was less than the measured mean minus 1 standard deviation.

Such high measurement precisions are essential for unequivocal identification of measurement-model discrepancies where CH_4 oxidation is the dominant source of CH_2O.

6. CH_2O Distributions and HO_x Production

6.1. CH_2O Distributions From Time-Coincident TDLAS and CDNPH Measurements

[42] Table 3 lists the ambient 5-min time-coincident CH_2O concentrations and associated statistics from both instruments for three different altitude ranges. Three different air mass types are presented according to the levels of various tracers. The cutoff limits were selected using histograms, which revealed clear distinctions between background and anthropogenically influenced conditions. Although the exact cutoffs for NO and NO_y might be open to question, the above limits should adequately capture all fresh and aged anthropogenic inputs, respectively. Like CO, C_2Cl_4 (lifetime of about 2 months) yields a good signature of continental plumes. Other hydrocarbons measured during NARE-97 could also be used; however, the number of such measurements (one measurement approximately every 15-min) would severely limit the number of observation points.

[43] As can be seen in Table 3, the maximum difference between corresponding means for the two instruments is 0.115 ppbv. However, most of the differences are well below 0.075 ppbv, as expected from the previous instrument comparison discussions. The data of Table 3 are also displayed in Figure 9 where all the 665 time-coincident measurements are plotted versus altitude. The dark larger points denote the median values in the three altitude bins, which decrease with altitude in both cases. As can be seen, the TDLAS and CDNPH systems measure significant amounts of CH_2O up to 1.88 ppbv and 1.55 ppbv, respectively, in the 0–2 km bin over the Atlantic Ocean off the North American continent. This occurred on September 16, 1997, where the flight track proceeded due south off the coast of New England (Figure 1, top). The median TDLAS and CDNPH CH_2O concentrations in the 0–2 km bin are 0.446 and 0.490 ppbv, respectively. These concentrations decrease minimally to 0.399 and 0.410 ppbv, respectively, when clean background conditions are selected.

[44] It is important to note that *Cohan et al.* [1999] indicate that convective pumping of CH_2O could be comparable in importance to H_2O_2 and CH_3OOH as a source of upper tropospheric HO_x if marine boundary layer CH_2O concentrations fall within the 0.6–1.0 ppbv range. *Jacob et al.* [1996] report that most models and observations in the tropical marine boundary layer fall within the 0.10–0.30 ppbv range, and thus transport of CH_2O in deep convection provides only a minor source of HO_x in the upper troposphere. This conclusion, however, is based on a very limited number of measurements. The results of the present study, which fall in the middle of the two ranges and closer to the upper range when all the data are considered, suggest that CH_2O in the marine boundary may indeed provide a greater contribution to upper tropospheric HO_x than previously thought. Despite the fact that deep marine convection is more prevalent in the tropics and the present measurements covered mid to high latitudes (35° to 55°N), one would expect that the 0.4–0.5 ppbv concentration range of this study would be significantly higher in the tropics. *Arlander et al.* [1995] observed such a trend during the TROPOZ II campaign. In the next section we will present additional TDLAS measurements acquired during the transit flight from St. Johns, Newfoundland, to Tampa, Florida, by which to further test the above assumption. However, it is important to first examine the present midlatitude time-coincident data set for evidence of elevated CH_2O concentrations in the upper troposphere due to vertical transport. As indicated previously, the flight locations and times were designed to sample synoptic midlatitude storms, which can readily redistribute boundary layer air vertically.

[45] Figure 10 displays all the time-coincident clean background measurements (Type II) from both instruments in the 4–8 km bin. As indicated in Table 3, the TDLAS and CDNPH instruments produce median values of 0.217 and 0.280 ppbv, respectively. The data were further parsed for dry and wet air masses to indicate the presence of recent vertical transport. The air mass was considered wet if the measured H_2O mixing ratio was greater than the mean mixing ratio, determined for each 0.5 km bin for the NARE campaign, plus 1 standard deviation. Likewise, dry air masses were selected where the measured H_2O mixing ratio was less than the measured mean minus 1 standard deviation. This produced median wet and dry H_2O mixing ratios of 3.2 and 0.23 g kg^{-1} for the 4–8 km range, respectively. The wet and dry measurements together comprise 50 to 55% of the clean background data acquired between 4 and 8 km, as intermediate H_2O mixing ratios are excluded in this analysis. In Table 4 we present the measurement statistics for the wet and dry air masses of Figure 10. It is interesting to note that the clean background wet CH_2O concentrations in the 4–8 km range of Table 4 in all cases are greater than the dry values, consistent with the potential importance of vertical transport in conveying marine boundary layer CH_2O to the upper troposphere. Laboratory tests carried out in the companion study by *Wert et al.* [2002] further indicate that the above TDLAS results are not produced by measurement artifacts either due to inlet effects or spectroscopic effects from a changing H_2O vapor broadening. Even under the wettest conditions of Table 4 or Table 6 (which shows the 1-min TDLAS measurements), the ambient H_2O vapor-mixing ratio was less than 1%. As discussed previously, calculations by *Fried et al.* [1998a] have shown that H_2O vapor mixing ratios as high as 2% do not affect the retrieved CH_2O mixing ratios in the 100 pptv range.

[46] Figure 10 and Table 4 reveal that both instruments show elevated levels of CH_2O up to 0.6 ppbv for the 4–8 km altitude range. Even the dry measurements, which presumably are not impacted by recent vertical transport, show CH_2O values up to 0.36–0.37 ppbv. By comparison, employing the steady state box model discussed in the companion paper by *Frost et al.* [2002], one calculates a diurnally averaged CH_2O concentration of 0.09 ppbv for this altitude range, which is a factor of 2 to 3 lower than the clean background measurements of Tables 3 and 4. *Frost et al.* [2002] will present a more detailed analysis of the measurement-model comparisons on a point-by-point basis. However, it is interesting to note that our measurement-model discrepancy is similar to that reported by *Arlander et al.* [1995], and this may suggest the presence of additional CH_2O precursors not presently being measured in the 4–8 km altitude range. *Frost et al.* [2002] will present additional possibilities for this discrepancy.

6.2. HO_x Production From CH_2O in the 4–8 km Range

[47] Regardless of the cause, assuming no instrumental errors, the elevated TDLAS and CDNPH CH_2O measurements in the 4–8

km altitude bin observed during the NARE campaign represent a significant source of HO_x radicals in the middle troposphere. The average of the TDLAS and CDNPH median CH_2O concentrations for all the time-coincident data (Type I) in the 4–8 km bin of Table 3 yields a value of 0.257 ppbv. This concentration in conjunction with a diurnally averaged radical photolysis frequency (R2a) of 1.4 $\times 10^{-5}s^{-1}$ yields a diurnally averaged HO_x production rate (P_{HOx}) of 1.0 $\times$ 10^5 molecules $cm^{-3}s^{-1}$ from CH_2O photolysis in accordance with

$$P_{HOx} = 2 \times \left(257 \times 10^{-12} \times 1.4 \times 10^{19} \text{ molecules cm}^{-3}\right) \times 1.4 \times 10^{-5}\text{s}^{-1} . \quad (1)$$

By comparison, the HO_x production rate from $O(^1D) + H_2O$ is 1.4 $\times$ 10^5 employing an average H_2O mixing ratio of 1.2 g kg^{-1}; from H_2O_2 photolysis is 4.5 $\times$ 10^4; and from a CH_3OOH photolysis is 1.6 $\times$ 10^4. These rates were calculated using expressions similar to equation (1) employing the appropriate diurnally averaged photolysis frequencies [see *Frost et al.,* 2002] and median measured concentrations values of 50, 0.493, and 0.231 ppbv for O_3, H_2O_2, and CH_3OOH, respectively, in the 4–8 km bin. Under these conditions the radical photolysis channel of CH_2O comprises 34% of the total HO_x production rate compared to 47% from $O^1D + H_2O$. However, in dry air in the 4–8 km bin the median CH_2O concentration for the two instruments averages 0.189 ppbv, while the H_2O vapor mixing ratio drops to a value of 0.23 g kg^{-1}. Under these conditions, CH_2O comprises 45% of the total HO_x production rate compared to 19% for the reaction $O^1D + H_2O$. It is clear from this analysis that the measurements from both instruments indicate that CH_2O provides a significant contribution to the middle tropospheric HO_x budget. The companion paper by *Frost et al.* [2002] further examines the net overall change in OH and HO_2 concentrations resulting from these observations.

6.3. CH_2O Distributions From 1-min TDLAS Measurements

[48] As indicated in the previous section, TDLAS measurements acquired during the return transit flight from St. Johns, Newfoundland, to Tampa, Florida, provide additional CH_2O measurements by which to expand our latitudinal coverage down to 28°N. The CDNPH instrument was not operated during the return transit flight. Rather than present only the transit flight TDLAS measurements, we present in this section all the 1-min measurements acquired by the TDLAS system during the NARE-97 campaign. Despite the fact that these measurements are less precise than the 5-min measurements, they expand the database from 665 to 3296 data points. These measurements are tabulated in Table 5 and displayed in Figure 11 in a similar fashion to those in Table 3 and Figure 9. A comparison of the two tables and two figures shows that a number of 1-min CH_2O measurements in the 0–2 km altitude bin were significantly greater than the 5-min measurements. Ambient CH_2O levels as high as 4.493 ppbv were measured during the return transit flight over Florida. As a result, the mean and median values in the 0–2 km bin for the total data set (Type I) and anthropogenically influenced data set (Type III) of Table 5 are slightly larger than the corresponding values of Table 3. All other corresponding values in the two tables fall within 0.033 ppbv of one another. The right- hand panel of Figure 11 again shows

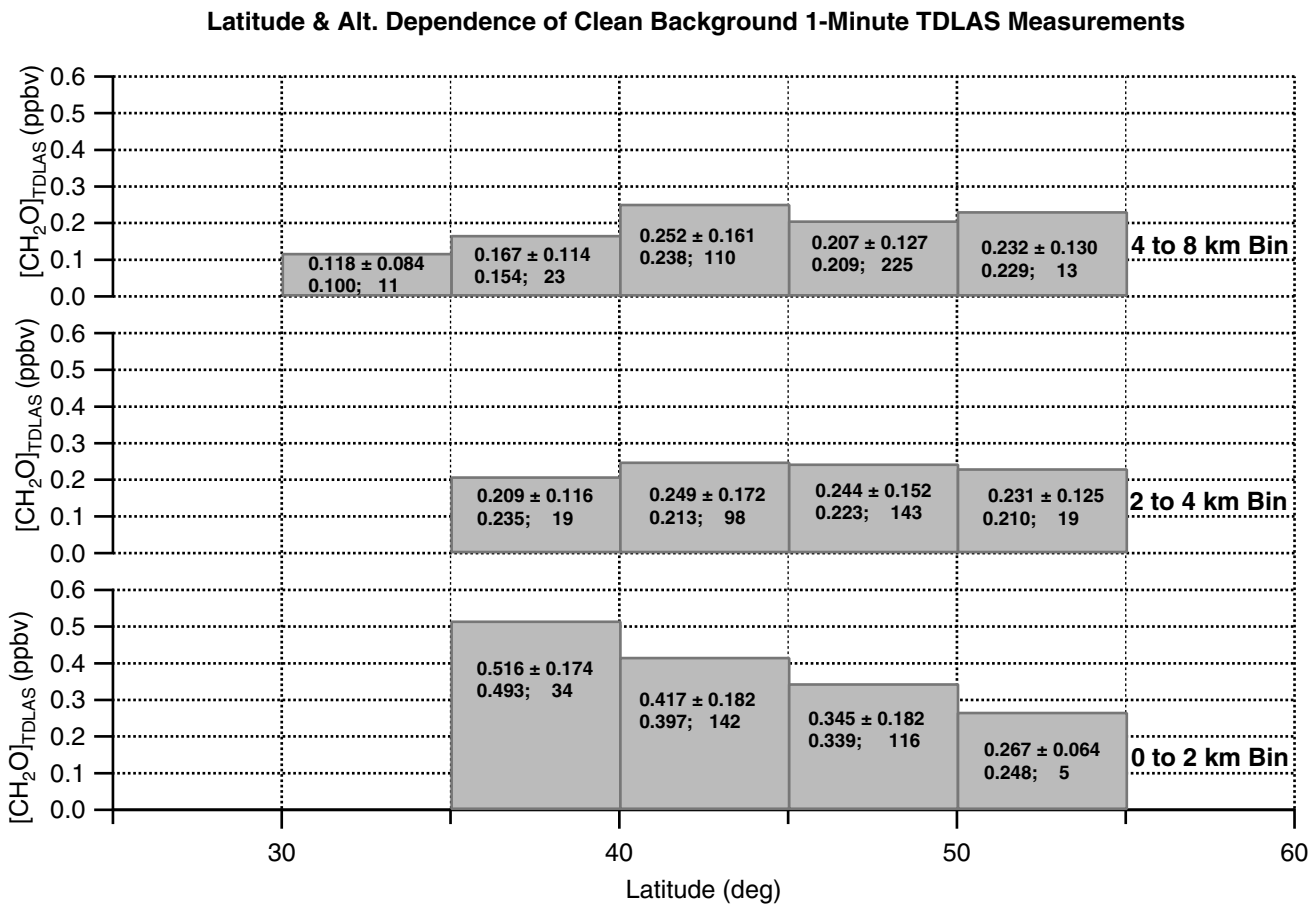

Figure 12. Latitudinal dependence of the clean background 1-min CH_2O measurements acquired by the TDLAS instrument for the three altitude regions. The data are binned into 5° latitude increments. The numbers in each box represent the mean and standard deviation, the median, and the number of measurements in each bin.

elevated clean background CH_2O measurements in the middle troposphere. Table 6, which tabulates the 1-min TDLAS measurements into wet and dry air masses, shows very similar results to the 5-min TDLAS measurements of Table 4.

[49] In Figure 12 we present the latitudinal dependence of the clean background 1-min TDLAS CH_2O data for the three altitude regions in 5° latitude increments. As can be seen, the background ambient CH_2O concentrations show a clear increase toward lower latitudes in the 0–2-km region, as expected from the increased temperature, and hence OH + CH_4 reaction rate, and the increased H_2O vapor with its consequent increased OH production rate. Marine biogenic sources of CH_2O, for example, from the oxidation of dimethyl sulfide, may also become more important at the lower latitudes. There is no corresponding obvious trend in the 2–4-km region, and a broad maximum in the 40°–55° latitude band in the 4–8-km region. The latter may reflect the influence of southerly vertical convection. Figure 12 indicates a median clean background CH_2O concentration of 0.493 ppbv in the 35°–40°N latitude bin for the 0–2-km range.

7. Comparisons With CH_2O Distributions From Other Measurement Campaigns

[50] As indicated in the introduction, there are numerous measurements of CH_2O, which have been carried out over continental and marine regions. We restrict our comparisons here to the 5-min time-coincident TDLAS and CDNPH measurements of Table 3 and the 1-min TDLAS measurements of Figure 12 with marine measurements from other studies carried out over the Atlantic on shipboard and aircraft platforms.

[51] The southbound airborne TROPOZ II measurements by *Arlander et al.* [1995] appear to be the most directly comparable with those of the present study since they were acquired over the same region off the coast of North America. The TROPOZ measurements indicated a broad CH_2O maximum at tropical latitudes at all altitudes and lower concentrations in the higher latitudes of the Northern Hemisphere [*Arlander et al.*, 1995]. The measurements of Figure 12 show this same latitudinal trend in the boundary layer but no obvious trend in the 2–4 km region and a weak reverse trend at higher altitudes. However, the TROPOZ measurements were not parsed to eliminate anthropogenic influence and were acquired during a different month (January) than the present measurements (September). Hence the degree of convective activity is likely to be different between the two studies. Such differences in turn could result in vastly different amounts of vertically convected CH_2O and its precursors to the mid and upper troposphere.

[52] In the boundary layer the 0.5 ppbv bin average for the 0–2 km, 30°–40°N, measurements of *Arlander et al.* [1995] is reasonably close to our nonparsed time-coincident (Type I) measurements of the present study in the same region. The 1-min TDLAS measurements average 0.631 ppbv for this region. This compares to our clean background measurements (Type II) of 0.516 ppbv, as shown in Figure 12. In the 2–4 km bin the nonparsed measurements of the present study between 35° and 55°N fall within the 0.3–0.4 ppbv range, with the clean background measurements about 0.05 ppbv lower. The two air mass types span the 0.28 ppbv average reported by *Arlander et al.* [1995] for this same region. In the 4–8 km region for 30°–50°N the agreement between the two studies is poorer. Our measurements in Table 3 yield CH_2O concentrations in the 0.2–0.3 ppbv range for both air mass types (I and II), while the *Arlander et al.* [1995] study reports concentrations around 0.1 ppbv at altitudes around 6 km and 0.05 ppbv at around 8 km. More detailed comparisons between the two studies not only need to factor in differences in meteorology but also differences in the temperature and light-dependent CH_2O production and destruction rates.

[53] *Weller et al.* [2000] report shipboard CH_2O measurements over the central Atlantic Ocean during the October/November 1996 Albatross campaign. Although median CH_2O concentrations around 0.4 ppb were observed between 35° and 50°N, in close agreement with our boundary layer measurements, the highest-latitude measurements around 0.1 ppbv at 50°N are about a factor of 2 lower than those of Figure 12. The TDLAS CH_2O measurements by *Harris et al.* [1992] during the September–October 1988 *Polarstern*cruise yield a mean mixing ratio of 0.47 ± 0.2 ppbv between 40° and 17°N, with a gradient toward lower values in the south of the measurement region. This mean value is very similar to our marine boundary layer values for the 35°–55°N region. By contrast, *Heikes et al.* [1996b], *Lowe and Schmidt* [1983], and *Junkermann and Stockwell* [1999] report significantly lower CH_2O levels in the 0.11–0.2 ppbv range in the clean tropical marine boundary layer.

8. Summary and Conclusions

[54] Airborne CH_2O measurements were made by tunable diode laser absorption spectroscopy (TDLAS) and coil/2,4-dinitrophenylhydrazine (CDNPH) techniques over remote regions of the North Atlantic Ocean from the surface to 8 km during the North Atlantic Regional Experiment (NARE-97) in September of 1997. There were eight aircraft flights when both instruments were simultaneously operating, and this produced 665 overlapping 5-min time intervals for comparison purposes. As the two techniques were based upon different measurement principles, calibration, and sampling approaches, the present study provides the first extensive comparison of two independent CH_2O techniques on board the same aircraft platform on a continuous basis.

[55] A number of approaches were used to compare the ambient CH_2O measurements acquired by the two instruments, including a weighted bivariate linear fit of all the time-coincident data as well as a subset of this data employing constant air mass legs, histograms of the measurement difference as a function of altitude and flight number for the complete and constant air mass data sets, and measurement differences averaged into 0.1 ppbv concentration bins as a function of concentration. The comparisons using the 665 time-coincident data set indicate that one or both instruments are less precise than anticipated. By contrast, the measurement difference during the 79 constant air mass periods produced a combined measurement precision of 0.117 ppbv, in reasonable agreement with that expected based upon the combined instrument precision.

[56] All the comparison analyses of this study indicated that on average the TDLAS and CDNPH instruments measured identical ambient CH_2O concentrations to within approximately 0.1 ppbv, and more typically within 0.08 ppbv, over the 0–0.8 ppbv-concentration range. However, significant differences, larger than the combined 2σ total uncertainty estimates, were observed in 29% of the full time-coincident data set.

[57] The two instruments produced very similar altitude trends during the NARE campaign. In the 0–2 km altitude range the TDLAS and CDNPH systems measured significant amounts of CH_2O up to 1.88 ppbv over the Atlantic Ocean off the North American continent when anthropogenically influenced air was sampled. However, under clean background conditions in the 35°–55°N latitude band, the median TDLAS and CDNPH CH_2O concentrations were 0.399 and 0.410 ppbv for 0–2 km, 0.250 and 0.355 ppbv for 2–4 km, and 0.217 and 0.280 ppbv for 4–8 km, respectively.

[58] Elevated CH_2O concentrations were observed in this study at both high altitudes (4–8 km) and in the marine boundary layer by both instruments. On the basis of a median CH_2O concentration of 0.257 ppbv for all the time-coincident data from both instruments in the 4–8 km bin (Type I air mass), the radical photolysis channel of CH_2O comprises 34% of the total HO_x production rate compared to 47% from $O^1D + H_2O$. This fraction increases to 45% of the total in dry air.

[59] The time-coincident 5-min measurements of the present study yield an average CH_2O concentration of 0.468 ppbv (the average of the median TDLAS and CDNPH measurements) in the marine boundary layer. Parsing for clean background conditions reduces this value to 0.405 ppbv. Both concentrations are very similar to those of *Arlander et al.* [1995], *Weller et al.* [2000], and *Harris et al.* [1992], which were carried out at similar latitudes over the North Atlantic. Background ambient 1-min TDLAS measurements in the 0–2 km bin show a clear increase toward lower latitudes. Between 35° and 40°N the 1-min data produce a median CH_2O concentration of 0.493 ppbv. We observed no obvious corresponding trend in the 2–4-km region, and a broad maximum in the 40°–55° latitude band in the 4–8-km region. The later may reflect the influence of southerly vertical convection.

[60] Finally, the use of two instruments employing entirely different measurement principles, calibration, and sampling approaches not only reinforces the above conclusions but also provides a high-quality database necessary to further explore CH_2O measurement-model relationships in the clean background atmosphere.

[61] **Acknowledgments.** The National Center for Atmospheric Research (NCAR) is sponsored by the National Science Foundation. The authors wish to acknowledge funding from NOAA's Climate and Global Change Program as well as contributions from Jack Fox and Steve Rauenbuehler at NCAR's machine and design group; Roger Hendershot and William Bradley at NCAR's electronic shop; Frank Flocke at NCAR for measurements of C_2Cl_4; Tom Ryerson, David Parrish, John Holloway, Roger Jakoubek, Donna Sueper, and Fred Fehsenfeld of the NOAA Aeronomy Laboratory for critical measurements and insightful discussions; and Mathew Evans for back trajectories.

References

Arlander, D. W., D. Brüning, U. Schmidt, and D. H. Ehhalt, The tropospheric distribution of formaldehyde during TROPOZ II, *J. Atmos. Chem.*, *22*, 251–268, 1995.

Ayers, G. P., R. W. Gillett, H. Granek, C. de Serves, and R. A. Cox, Formaldehyde production in clean marine air, *Geophys. Res. Lett.*, *24*, 401–404, 1997.

Bethan, S., G. Vaughan, C. Gerbig, A. V. Thomas, H. Richer, and D. A. Tiddeman, Chemical air mass differences near fronts, *J. Geophys. Res.*, *103*, 13,413–13,434, 1998.

Calvert, J. G., R. Atkinson, S. Kerr, G. K. Madronich, G. Moortgat, T. J. Wallington, and G. Yarwood, *The Mechanisms of Atmospheric Oxidation of the Alkenes*, pp. 371–379, Oxford Univ. Press, New York, 2000.

Carlier, P., H. Hannachi, and G. Mouvier, The chemistry of carbonyl compounds in the atmosphere: A review, *Atmos. Environ.*, *20*, 2079–2099, 1986.

Cohan, D. S., M. G. Schultz, D. J. Jacob, B. G. Heikes, and D. R. Blake, Convective injection and photochemical decay of peroxides in the tropical upper troposphere: Methyl iodide as a tracer of marine convection, *J. Geophys. Res.*, *104*, 5717–5724, 1999.

DeMore, W. B., S. P. Sander, D. M. Golden, R. F. Hampson, M. J. Kurylo, C. J. Howard, A. R. Ravishankara, C. E. Kolb, and M. J. Molina, Chemical kinetics and photochemical data for use in stratospheric modeling, Evaluation number 12, *JPL Publ.*, *97-4*, 1997.

de Serves, C., Gas phase formaldehyde and peroxide measurements in the Arctic atmosphere, *J. Geophys. Res.*, *99*, 25,391–25,398, 1994.

Dong, S., and P. K. Dasgupta, Solubility of gaseous formaldehyde in liquid water and generation of trace standard gaseous formaldehyde, *Environ. Sci. Technol.*, *20*, 637–640, 1986.

Fried, A., S. Sewell, B. Henry, B. P. Wert, T. Gilpin, and J. R. Drummond, Tunable diode laser absorption spectrometer for ground-based measurements of formaldehyde, *J. Geophys. Res.*, *102*, 6253–6266, 1997a.

Fried, A., et al., Photochemistry of formaldehyde during the 1993 Tropospheric OH Photochemistry Experiment, *J. Geophys. Res.*, *102*, 6283–6296, 1997b.

Fried, A., B. Henry, B. Wert, S. Sewell, and J. R. Drummond, Laboratory, ground-based, and airborne tunable diode laser systems: Performance characteristics and applications in atmospheric studies, *Appl. Phys. B*, *67*, 317–330, 1998a.

Fried, A., B. P. Wert, B. Henry, and J. R. Drummond, Airborne tunable diode laser measurements of trace atmospheric gases, *Proc. SPIE Int. Soc. Opt. Eng.*, *3285*, 154–162, 1998b.

Fried, A., B. Wert, B. Henry, J. R. Drummond, G. Frost, and Y.-N. Lee, Airborne tunable diode laser measurements of formaldehyde during the 1997 North Atlantic Regional Experiment, *Proc. SPIE Int. Soc. Opt. Eng.*, *3758*, 90–99, 1999.

Frost, G. J., et al., Comparisons of box model calculations and measurements of formaldehyde from the 1997 North Atlantic Regional Experiment, *J. Geophys. Res.*, 10.1029/2001JD000896, in press, 2002.

Gilpin, T., et al., Intercomparison of six ambient [CH_2O] measurement techniques, *J. Geophys. Res.*, *102*, 21,161–21,188, 1997.

Grosjean, E., E. L. Williams II, and D. Grosjean, Ambient levels of formaldehyde and acetaldehyde in Atlanta, Georgia, *J. Air Waste Manage. Assoc.*, *43*, 469–474, 1993.

Harder, J. W., A. Fried, S. Sewell, and B. Henry, Comparison of tunable diode laser and long path ultraviolet/visible spectroscopic measurements of ambient formaldehyde concentrations during the 1993 OH Photochemistry Experiment, *J. Geophys. Res.*, *102*, 6267–6282, 1997.

Harris, G. W., D. Klemp, T. Zenker, and J. P. Burrows, Tunable diode laser measurements of trace gases during the 1988 Polarstern Cruise and intercomparisons with other methods, *J. Atmos. Chem.*, *15*, 315–326, 1992.

Heikes, B. G., Formaldehyde and hydroperoxides at Mauna Loa Observatory, *J. Geophys. Res.*, *97*, 18,001–18,013, 1992.

Heikes, B. G., et al., Formaldehyde methods comparison in the remote lower troposphere during the Mauna Loa Photochemistry Experiment 2, *J. Geophys. Res.*, *101*, 14,741–14,755, 1996a.

Heikes, B. G., M. Lee, D. Jacob, R. Talbot, J. Bradshaw, H. Singh, D. Blake, B. Anderson, H. Fuelberg, and A. M. Thompson, Ozone, hydroperoxides, oxides of nitrogen, and hydrocarbon budgets in the marine boundary layer over the South Atlantic, *J. Geophys. Res.*, *101*, 24,221–24,234, 1996b.

Jacob, D. J., et al., Origin of ozone and NO_x in the tropical troposphere: A photochemical analysis of aircraft observations over the South Atlantic basin, *J. Geophys. Res.*, *101*, 24,235–24,250, 1996.

Jaeglé, L., et al., Photochemistry of HO_x in the upper troposphere at northern midlatitudes, *J. Geophys. Res.*, *105*, 3877–3892, 2000.

Junkermann, W., and W. R. Stockwell, On the budget of photooxidants in the marine boundary layer of the tropical South Atlantic, *J. Geophys. Res.*, *104*, 8039–8046, 1999.

Lee, M., B. G. Heikes, D. J. Jacob, G. Sachse, and B. Anderson, Hydrogen peroxide, organic hydroperoxide, and formaldehyde as primary pollutants from biomass burning, *J. Geophys. Res.*, *102*, 1301–1309, 1997.

Lee, Y.-N., and X. Zhou, Method for the determination of some soluble atmospheric carbonyl compounds, *Environ. Sci. Technol.*, *27*, 749–756, 1993.

Lee, Y.-N., X. Zhou, W. R. Leaitch, and C. M. Banic, An aircraft measurement technique for formaldehyde and soluble carbonyl compounds, *J. Geophys. Res.*, *101*, 29,075–29,080, 1996.

Lee, Y.-N., et al., Atmospheric chemistry and distribution of formaldehyde and several multioxygenated carbonyl compounds during the 1995 Nashville/Middle Tennessee Ozone Study, *J. Geophys. Res.*, *103*, 22,449–22,462, 1998.

Liu, S. C., et al., A study of the photochemistry and ozone budget during the Mauna Loa Observatory Photochemistry Experiment, *J. Geophys. Res.*, *97*, 10,463–10,471, 1992.

Lowe, D. C., and U. Schmidt, Formaldehyde (HCHO) measurements in the nonurban atmosphere, *J. Geophys. Res.*, *88*, 10,844–10,858, 1983.

McConnell, J. C., M. B. McElroy, and S. C. Wofsy, Natural sources of CO, *Nature*, *233*, 187–188, 1971.

Neitzert, V., and W. Seiler, Measurement of formaldehyde in clean air, *Geophys. Res. Lett.*, *8*, 79–82, 1981.

Neri, F., G. Saitta, and S. Chiofalo, An accurate and straightforward approach to line regression analysis of error-affected experimental data, *J. Phys. E Sci. Instrum.*, *22*, 215–217, 1989.

Platt, U., D. Perner, and H. W. Pätz, Simultaneous measurement of atmospheric CH_2O, O_3, and NO_2 by differential optical absorption, *J. Geophys. Res.*, *84*, 6329–6335, 1979.

Rothman, L. S., et al., The HITRAN molecular spectroscopic database and HAWKS (HITRAN Atmospheric Workstation): 1996 edition, *J. Quant. Spectrosc. Radiat. Transfer*, *60*, 665–710, 1996.

Sewell, S., A. Fried, B. Henry, and J. R. Drummond, A field diode laser spectrometer employing an astigmatic Herriott cell, *Proc. SPIE Int. Soc. Opt. Eng.*, *2112*, 72–80, 1993.

Sigsby, J. E., S. Tejada, W. Ray, J. M. Lang, and J. W. Duncan, Volatile organic compound emissions from 46 in-use passenger cars, *Environ. Sci. Technol.*, *21*, 466–475, 1987.

Singh, H., et al., High concentrations and photochemical fate of oxygenated hydrocarbons in the global troposphere, *Nature*, *378*, 50–54, 1995.

Weller, R., O. Schrems, A. Boddenberg, S. Gäb, and M. Gautrois, Meridional distribution of hydroperoxides and formaldehyde in the marine boundary layer of the Atlantic (48°N-35°S) measured during the Albatross campaign, *J. Geophys. Res.*, *105*, 14,401–14,412, 2000.

Wennberg, P. O., et al., Hydrogen radicals, nitrogen radicals, and the production of O_3 in the upper troposphere, *Science*, *279*, 49–53, 1998.

Wert, B. P., A. Fried, B. Henry, and J. R. Drummond, Airborne measurements of tropospheric formaldehyde by tunable diode laser absorption spectroscopy, *Proc. SPIE Int. Soc. Opt. Eng.*, *2834*, 175–186, 1996.

Wert, B. P., A. Fried, B. Henry, and J. R. Drummond, Enhancement of a tunable diode laser tropospheric trace gas measurement system, *Proc. SPIE Int. Soc. Opt. Eng.*, *3758*, 100–108, 1999.

Wert, B. P., A. Fried, B. Henry, and S. Cartier, Evaluation of inlets used for the airborne measurement of formaldehyde, *J. Geophys. Res.*, 10.1029/2001JD001072, in press, 2002.

Zafiriou, O. C., J. Alford, M. Herrera, E. T. Peltzer, R. B. Gagosian, and S. C. Liu, Formaldehyde in remote marine air and rain: Flux measurements and estimates, *Geophys. Res. Lett.*, *7*, 341–344, 1980.

Zhou, X., Y.-N. Lee, L. Newman, X. Chen, and K. Mopper, Tropospheric formaldehyde concentration at the Mauna Loa Observatory during the Mauna Loa Observatory Photochemistry Experiment 2, *J. Geophys. Res.*, *101*, 14,711–14,719, 1996.

J. R. Drummond, Department of Physics, University of Toronto, Toronto, Ontario, Canada M5S 1A7.

A. Fried, B. Henry, and B. Wert, National Center for Atmospheric Research, Boulder, CO 80303, USA. (fried@acd.ucar.edu)

G. Frost, G. Hübler, and T. Jobson, Aeronomy Laboratory, NOAA, Boulder, CO 80303, USA.

Y.-N. Lee, Brookhaven National Laboratory, Upton, NY 11973, USA.